Application of Supercontinuum Generation to Practical Absorption Spectroscopy

by

Jonathan A. Filipa

A thesis submitted in partial fulfillment of

the requirements for the degree of

Master of Science

(Mechanical Engineering)

at the

UNIVERSITY OF WISCONSIN-MADISON

2005

ABSTRACT

Application of Supercontinuum Generation to Practical Absorption Spectroscopy

Jonathan A. Filipa

Under the supervision of Assistant Professor Scott T. Sanders

At the University of Wisconsin-Madison

Supercontinuum light generation was used as a means to generate broadband light for spectroscopic measurements. The generated broadband light was used to measure carbon monoxide (CO) absorption in a sealed laboratory test cell. This investigation served as a proof of concept for optical system development that in the future can be applied towards making combustion measurements.

Some of the basic concepts underlying supercontinuum generation are reviewed and the advantages and disadvantages of this broadband light generation technique are discussed. Particularly, interference brought on by the propagation of broadband light is reviewed and methods to deal with it are discussed. The distinction between high and low quality light for making spectroscopic measurements is detailed and CO absorption measurements were made using both types of light. From reviewing the results, it was found that high quality light is superior to low quality light for making high-speed spectroscopic measurements.

ACKNOWLEDGEMENTS

First of all I have to thank my advisor, Professor Scott Sanders, for giving me the opportunity to study at the University of Wisconsin as a part of the Engine Research Center. Dr. Sanders and Dr. Joachim Walewski have both been invaluable for their guidance of my research and their advice and availability on a day-to-day basis greatly enhanced my learning during my time in graduate school.

I have to thank my fellow students in the Sanders' research group for their friendship and advice with issues around the lab. Working with such good people made life a lot more enjoyable both in and out of the office and I want to wish everyone the best in their future endeavors.

Ralph Braun is due a big thanks for his help around the machine shop and his advice on after-hours projects as well.

I must acknowledge the United States Department of Energy for funding my research project through US DOE Cooperative Agreement DE-FC2602NT41431 under UTSR project 03-01-SR105.

Lastly and most importantly, I have to thank my family for their continual support during my time in graduate school as I would not be where I am today without them.

TABLE OF CONTENTS

LIST OF FIGURES

LIST OF EQUATIONS

CHAPTER 1 – MOTIVATION AND BACKGROUND

1.1 Motivation

It is possible to use optical systems to measure gas temperature, pressure, and species mole fractions in an engine. Electromagnetic radiation (light) that is sent through a combustion chamber will be absorbed by the various species present in the chamber and the absorption spectra that are measured can be used to infer relevant properties about the engine in an accurate, highly time-resolved fashion. A schematic of an optical system that could be used for engine measurements is shown below in Figure 1.1.

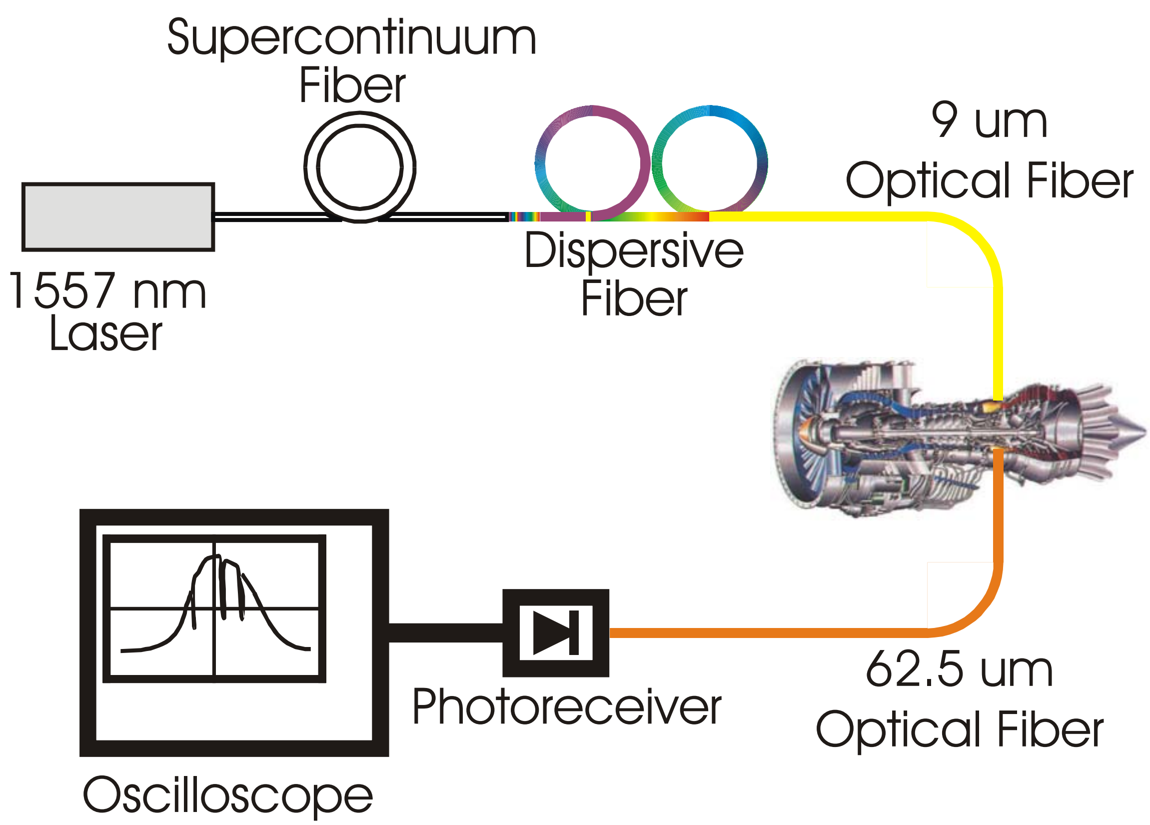

Figure 1.1. Optical system for combustion measurements

The laser, the supercontinuum fiber, and the dispersive fiber would be used to create high resolution broadband light which would go through 9 μm diameter optical fiber into a combustion environment. The type of engine shown in Figure 1.1 is a jet engine, but it could also be a piston engine or a rocket engine as all that is needed is optical access to the region of interest for any type of engine. After the engine, light is collected in a larger 62.5 μm diameter optical fiber and sent to an optical receiver such as a photodiode which is connected to an oscilloscope for digital collection and processing of the data.

Recent work at the University of Wisconsin Engine Research Center has produced optical sensors that are capable of measuring water absorption in piston engines. Some representative data is shown in Figure 1.2.

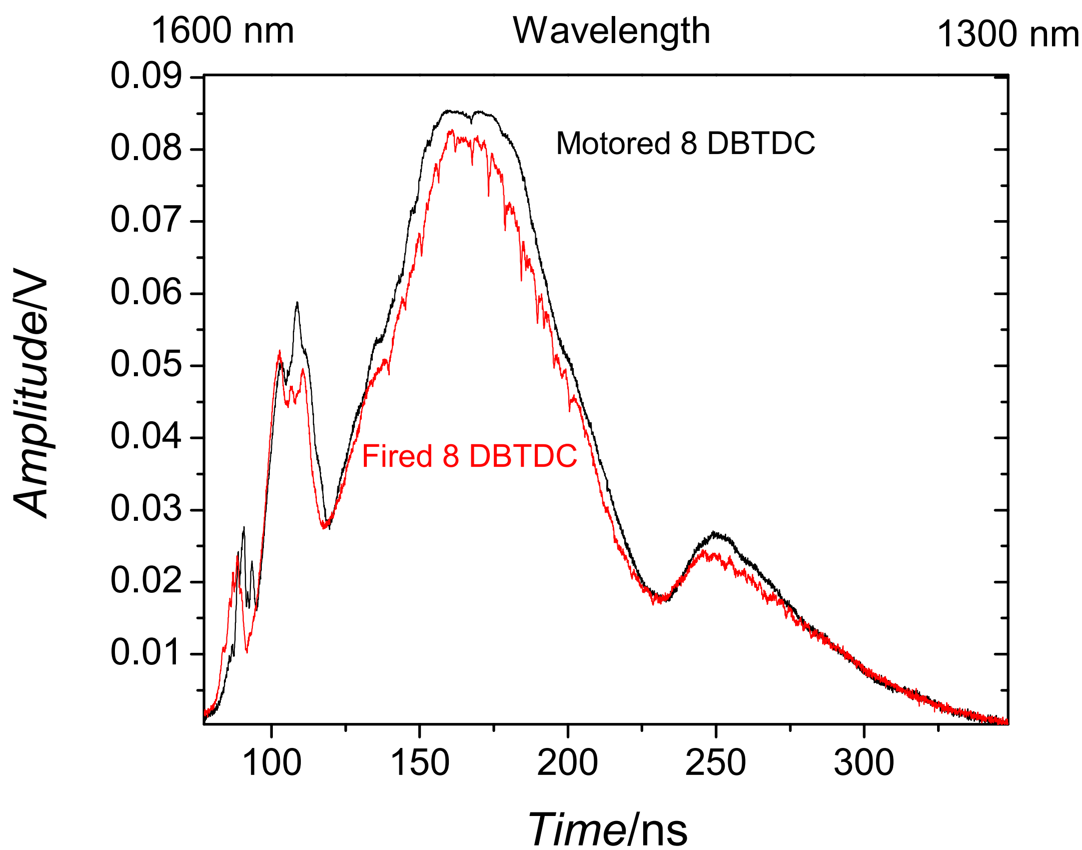

Figure 1.2. Water absorption in an HCCI engine

The black trace was recorded while the engine was being turned over by a dynamometer and not fired and was recorded to serve as a baseline for comparison. The red trace was recorded while the engine was being run in HCCI (homogeneous charge compression ignition) mode. More general information on HCCI combustion is available elsewhere [1], [2, 3]. From comparing the red trace to the black trace, it is seen that the two traces have almost the same exact shape but the red trace has a slight overall attenuation (slight decrease in amplitude) and also has several very narrow lines in the recorded signal. These narrow lines are localized decreases in amplitude and are a result of water vapor in the product gases absorbing specific wavelengths of the light as the light was directed through the cylinder. These absorption lines are the key pieces of information in this figure and can be used to infer temperature, pressure, and mole fraction at the instant in time the data was recorded.

Research is continuing in optical diagnostics because optical systems have a much faster time response than traditional experimental means such as thermocouples and also have the capability to be more accurate because they do not physically intrude into the test environment. This paper will review necessary background information and some experimental techniques for making practical absorption spectroscopy measurements in applications such as piston engines, gas turbines, and rocket engines.

1.2 Absorption Spectroscopy of Gases

Absorption spectroscopy is a growing field that uses optical techniques to measure changes in quantum states for a given substance or substances. Absorption occurs when a molecule or atom changes quantum states from a lower energy state to a higher energy state and in the process absorbs a photon [4]. For most absorption measurements the substances being measured are pumped with a laser and it should be noted that typically the incident laser signal is tracked using detection equipment so the increase in energy due to absorption in a species is seen as a decrease in energy in the laser signal. For clarification, all work for this paper was done with gases so it will be assumed that any reference to substances, elements, molecule, or atoms will be for their gaseous state.

Absorption is calculated by taking the natural logarithm of the negative quotient of the absorbed light (I) divided by the unabsorbed light (I_o). This is referred to as Beer's Law. In equation form,

$$Absorption = -\ln\left(\frac{I}{I_o}\right)$$

Equation 1.1. Beer's Law for absorption

Figure 1.3 shows broadband LED light being sent through a cell with no acetylene (black trace) and with acetylene (red trace).

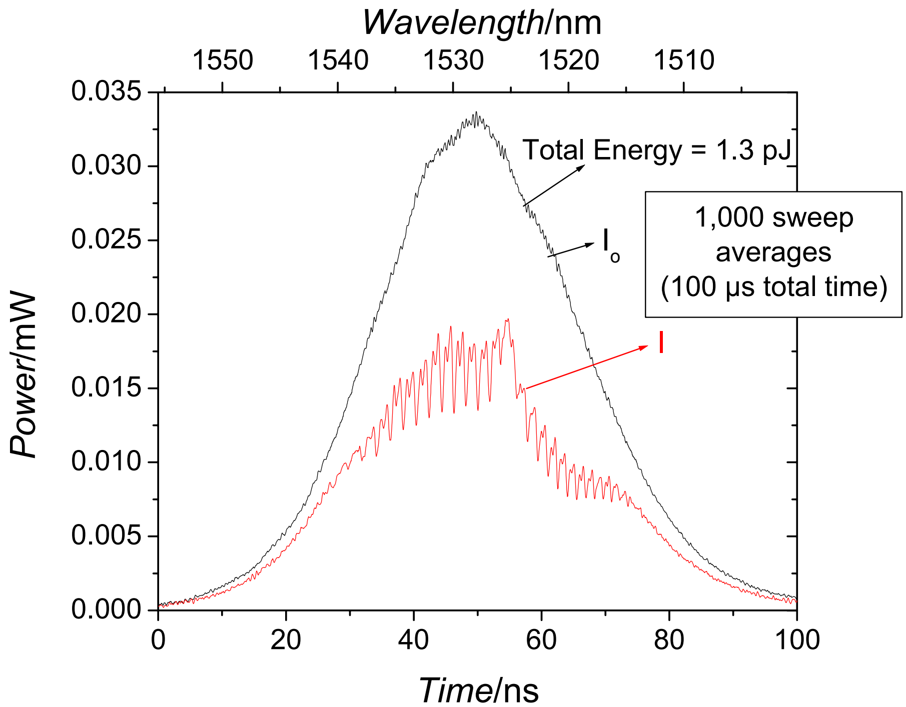

Figure 1.3. Laser spectrum with and without acetylene absorption

It can be seen that acetylene produces a strong overall attenuation of the light as well as narrow, localized decreases in amplitude at individual wavelengths which give acetylene its unique absorption profile. Molecules and atoms absorb light at specific, repeatable energy levels for a given temperature and pressure which in turn yield a specific, repeatable wavelength absorbance (the terms absorption and absorbance mean the same thing) pattern for a given species and ambient environment. Figure 1.4 shows absorbance versus wavelength calculated from the same acetylene data.

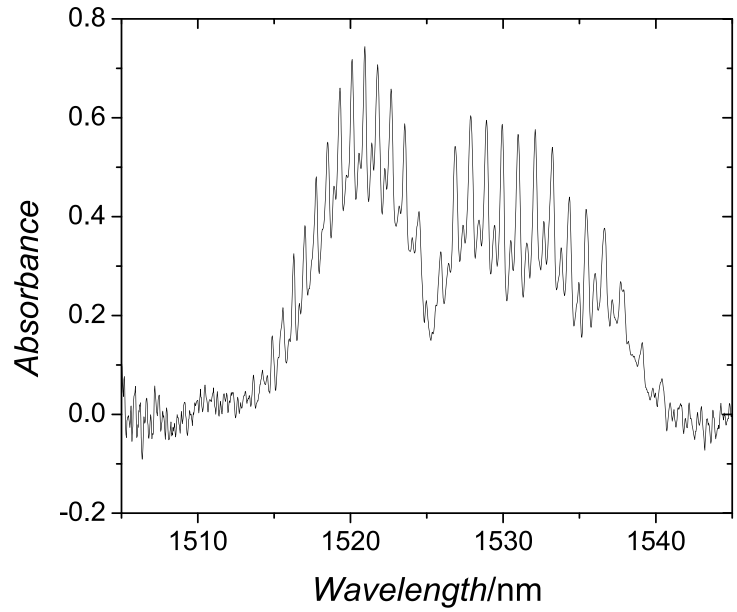

Figure 1.4. Acetylene absorption

From the plot it is seen that acetylene has two definite branches in its absorption spectrum which is typical for most substances. As can be seen in Figures 1.3 and 1.4, the data was taken as power versus time and converted to absorbance versus wavelength. As both the absorbed (I) and unabsorbed signals (I_o) were measured for this test calculating the absorbance was straightforward. Converting the time axis to wavelength required comparing the calculated absorbance to the known acetylene absorption spectrum and developing a linear relationship between the recorded time and the known wavelengths.

Absorption lines have both a temperature and pressure dependence. Temperature changes the relative strength of absorption lines. This is shown in Figure 1.5.

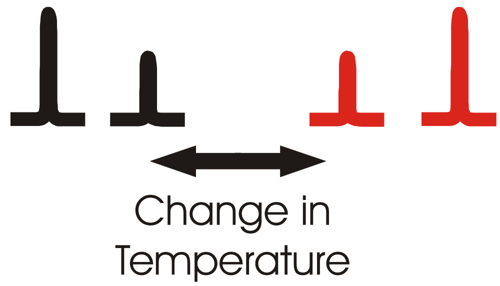

Figure 1.5. Absorption temperature dependence

Species often have “hot” or “cold” absorption lines meaning that certain wavelengths absorb more light at higher temperatures and other wavelengths absorb more light at lower temperatures. Pressure affects the width of individual absorption lines as increasing pressure increases the width of absorption lines as shown in Figure 1.6 while a decrease in pressure does the opposite.

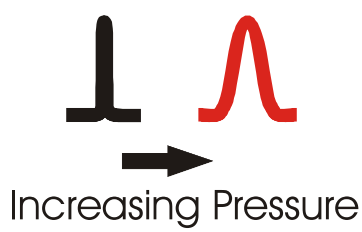

Figure 1.6. Absorption pressure dependence

Absorption spectroscopy can be used for extremely high speed measurements where the limiting time response factor typically would be the response time of the detection equipment, usually a photoreceiver and oscilloscope. Numerous “snapshots” of the absorbed light would be recorded with the photoreceiver and oscilloscope and saved for data processing, much like was done for Figures 1.1 and 1.2 but done multiple times. As absorption is calculated from the ratio of the absorbed light divided by the unabsorbed signal, each snapshot of the absorbed light would need its own unabsorbed data trace to calculate absorption at each instance in time. Since absorption lines are very narrow, often times all that is done to form an I_o (unabsorbed trace) is to interpolate over the absorption lines as if they were never there as shown in Figure 1.7.

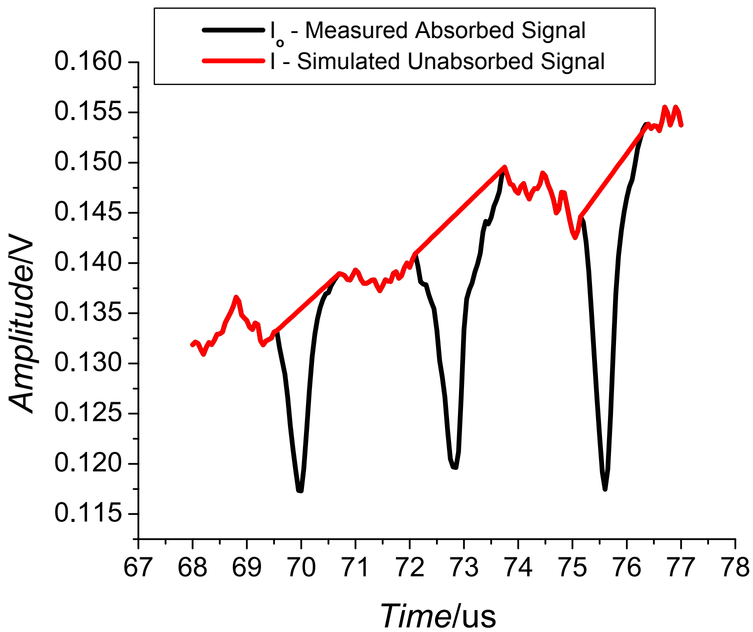

Figure 1.7. Fitting of unabsorbed trace to absorbed data

Once an appropriate method for determining I_o (unabsorbed) is specified it will need to be applied for each I (absorbed) trace to calculate absorbance for each individual piece of data. Converting the time axis to wavelength will need to be done in the same manner as described earlier. This will result in a conversion of amplitude versus time to absorption versus wavelength while maintaining the same accuracy as the raw signal. Once this is done, each snapshot of absorption versus wavelength can be compared to known spectral databases to determine temperature and pressure for each individual data set.

As referred to previously, different atoms and molecules have unique quantum structures which result in unique absorption properties for a given substance. This allows for the measurement of multiple species at the same time and gives absorption spectroscopy a very high utility as a measurement technique. As long as the species of interest have absorption bands that do not overlap the only things limiting the number of compounds or elements that can be measured are the bandwidth of the light source and the optical transmission characteristics of the system.

1.2.1 Relevant Properties Needed to Determine Wavelength-scan Method

As mentioned above, wavelength scan range is an important parameter that needs to be considered when trying to determine an approach for generating a wavelength scan. The ability to track more absorption lines for one or more species yields more information and improves the accuracy of the system.

Another important property of optical systems that needs to be looked at for any spectral measurement is the spectral resolution of the system. Spectral resolution refers to the smallest wavelength increment where changes can be tracked by the system. Having as small a spectral resolution as possible is always desirable, and it is definitely necessary to have a spectral resolution that is smaller than the linewidth of a typical absorption line for the species of interest. Absorption line linewidth depends on the given conditions. For example, water absorption lines have a linewidth of 0.4 nm (2 cm^{-1}) at a pressure of 10 bar and a temperature of 294 K. The linewidth of water lines at combustion conditions is still somewhat unknown, as a linewidth of approximately 0.18 nm (0.9 cm^{-1}) is expected for 10 bar, 1540 K but recent simulations have yielded a linewidth of 0.06 nm (0.3 cm^{-1}) for the same conditions. Future work should hopefully clear this up.

The last property that should be addressed when selecting a system for spectroscopic measurements is the scan repetition rate of the system, essentially how fast data can be collected. This is something that should be as high as possible and modern optical systems have repetition rates that extend well into the kilohertz range (kHz) and sometimes the megahertz (MHz) range. Many times it is necessary when making optical measurements to average the data to improve the signal-to-noise ratio which decreases the overall scan repetition rate. The scan rate is then inversely proportional to the number of averages employed.

Wavelength scan range, spectral resolution, and scan repetition rate all should be looked into when trying to decide which type of optical system to use for an experimental measurement and a lot of times one method will do well in one area but will not be acceptable in one or both of the other two. Careful attention needs to be paid to what specifications are necessary to get acceptable data when trying to select an appropriate wavelength-scan method.

1.3 Combustion Applications for Spectroscopy

Spectroscopy lends itself well to making combustion measurements as it is a non-intrusive measurement technique. Being non-intrusive is crucial for making accurate, high fidelity measurements of combustion as inserting probes into a highly chaotic, turbulent fluid flow can easily disturb the flow to a point where the measured properties lose any relation to what would be going on in a non-instrumented device. Optical measurements of course require optical access to the combustion chamber of interest and this is usually done by putting windows on each side of the chamber. Incorporating windows makes a test engine slightly different than a production engine but two small windows is still a lot closer to production that inserting probes or thermocouples into an engine or modifying spark plugs. Figure 1.8 is a picture of an engine ring that is equipped with sapphire windows and optical fiber mounting stages.

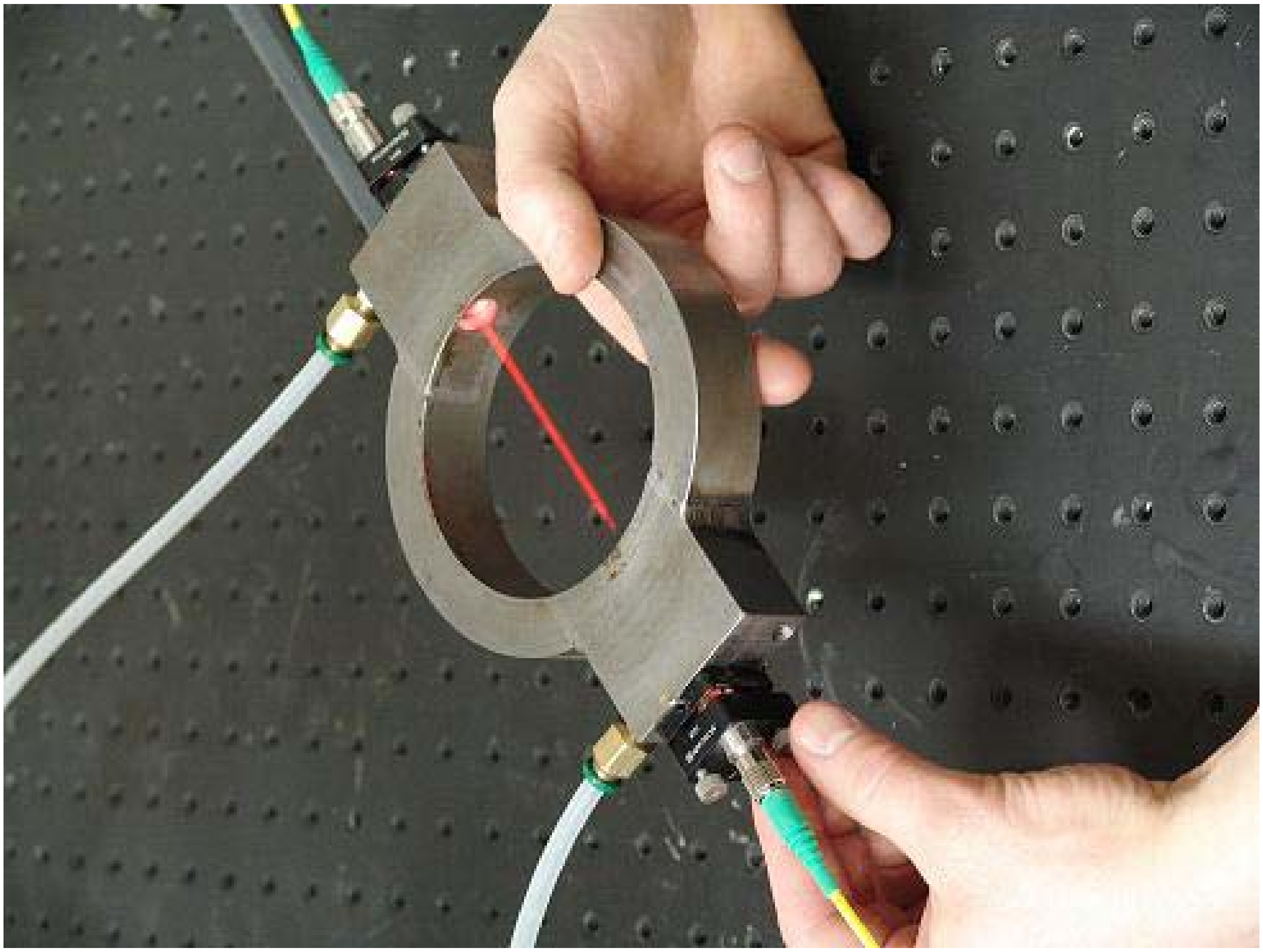

Figure 1.8. Ring for piston engine with optical fiber mounting stages

This engine ring is designed to fit between the cylinder and head on a single cylinder test engine and allows access to the combustion chamber with minimal intrusion.

Being able to have all of your optical equipment outside of the combustion chamber is also advantageous as compared to conventional mechanical thermocouples and pressure transducers because combustion environments are extremely harsh and can easily damage any type of sensor present in the chamber. So, having a non-invasive sensor will almost always increase the reliability of the detection equipment and reduce the chance of damaging a test engine due to a sensor breaking off in the combustion chamber.

When talking about making combustion measurements, optical techniques have been used to measure temperature, pressure, and other properties in piston engines, gas turbines, and rocket engines. All that is required is proper optical access to the combustion chamber or other possible areas of interest in the engine.

1.3.1 Accuracy and Response Time for a Typical Mechanical Pressure Transducer

A typical pressure transducer used for combustion measurements is a Kistler Type 6125B ThermoComp Quartz Pressure Sensor. This device has a pressure range of 0 to 250 bar and a calibrated partial range from 0 to 50 bar. When combined with a Kistler 5010B dual mode charge amplifier, this setup would have an accuracy of 0.5% and a time constant as small as 0.1 s [5].

1.3.2 Accuracy and Response Time for a Typical Mechanical Thermocouple

A typical thermocouple used to measure flow properties for combustion measurements (intake charge temperature, exhaust gas temperature) is an Omega Type K thermocouple. This device has a range of -200 ^{o}C to 1250 ^{o}C which typically does not allow for direct measurement of flame temperature. This thermocouple has an accuracy of 2.2 ^{o}C or 0.75% (whichever is larger) and a response time of 0.25 s to 2.25 s depending on the probe's diameter [5].

1.4 Previous Work

Much work has been done and a lot of progress has been made in absorption spectroscopy for combustion applications in the past quarter century and the references listed in this paper are a very small sample of what is available in published literature.

1.4.1 Wavelength-agile Absorption Spectroscopy

Building on initial measurements of simple flames [6], it soon became apparent that sources with a wider spectral bandwidth and faster tuning capabilities (wavelength-agile sources) were necessary for making measurements in practical, high-pressure combustion systems.

Vertical-cavity surface-emitting lasers (VCSELs) emerged approximately five years ago with a tuning wavelength range approximately 20 times that of standard distributed-feedback (DFB) diode lasers which could be scanned in 1/100th the time [7]. VCSELs were successful in making measurements in harsh environments but are limited in use due to the relative lack of commercial availability above wavelengths of 1000 nm. Another issue with VCSELs is the large thermal swings that result from trying to rapidly tune wavelength. VCSEL measurements are well-documented and the reader is encouraged to find other information and references [8].

Another type of optical sensor that has emerged involves the utilization of a scanning mirror. Light from a broadband source such as an LED is directed off of a diffraction grating which disperses the light in space. This dispersed light is then reflected off of a rapidly vibrating mirror which slightly rotates the light as the mirror moves. The moving light is directed through a narrow iris which only lets though a narrow portion of the dispersed wavelength band at each instance in time. This sliced light can then be routed to an engine for gas measurement. The limiting factor for the scanning mirror approach is the vibration frequency of the mirror (on the order of 10 kHz) which limits the wavelength scan speed of the system [8]. More detailed information and experimental results using the scanning mirror approach can be found elsewhere [2].

Chirped white pulse emitters (CWPEs) are another type of sensor that utilize wavelength-agility. The idea behind CWPEs is to disperse short duration, broadband optical pulses in a highly dispersive medium such that the individual colors spread out spatially so that they can be tracked with high resolution using a high-speed photoreceiver connected to a high-speed oscilloscope. Often times it is much more convenient to use an optical fiber with a high dispersion instead of other means for dispersion (bulk material, multiple reflections) and more information on fiber dispersion is available for the interested reader [9]. The resolution for this type of system is strictly dependant on the pulse duration of the laser and the net dispersion of the system. The measurement frequency for CWPEs is the simply the repetition frequency of the laser. One issue to keep in mind with this system is that

CWPEs often require very long dispersion fibers (often times several kilometers) which results in high attenuation of the light (sometimes 99% or more), especially when utilizing wavelengths significantly away from the minimum attenuation band at 1550 nm for silica telecommunications fibers. One recent effort with a CWPE system was found to be sufficient to resolve individual rotational lines for acetylene (C_2H_2). This system employed an 18 km dispersion fiber, had a resolution of 0.40 cm-1, had 5 pJ/pulse available at the photodiode detector, and had a repetition rate of 50 MHz [10]. The reader is encouraged to investigate the paper referenced for more information on the experimental setup and results.

1.4.2 Supercontinuum

Supercontinuum light generation has been demonstrated in optical fibers. In one case, an optical spectrum ranging from 1.1 to 2.1 μm was achieved using a mode-locked erbium-doped fiber laser and a polarization maintaining highly nonlinear dispersion shifted fiber. It was found that bandwidth increased with an increase in power and increasing fiber length caused the supercontinuum spectrum to flatten out [11].

Standard telecommunication fibers have been used as mediums for supercontinuum generation [12]. Typical telecommunications fibers are attractive because they are relatively inexpensive and are easier to integrate into experimental systems than specialized highly nonlinear fibers. It was seen that usable supercontinuum generation was achieved in Corning SMF-28 fiber, Fujikura Dispersion

Compensation Fiber, and Corning Metrocor fiber. Issues such as material nonlinear coefficient, absolute fiber dispersion, positive or negative dispersion, and fiber damage threshold were found to be key issues in selecting an appropriate fiber for supercontinuum applications.

Supercontinuum light generation has been used for measuring absorption of H_2O, CO_2, and C_2H_2 simultaneously [13]. For this measurement, light from an erbium-doped fiber laser was propagated through a non-linear fiber and a dispersion-shifted fiber to achieve a usable wavelength scan from 1350 to 1550 nm. The scan rate for this system was approximately 200 nm every 20 ns, which is roughly four orders of magnitude greater than some other well-known time-of-flight spectroscopic methods.

CHAPTER 2 – SUPERCONTINUUM LIGHT GENERATION

2.1 Theory

Supercontinuum light generation is a self-phase modulation phenomenon that relies heavily on nonlinear processes occurring in the propagation medium. The energy density of the light and the nonlinear coefficient of the propagation medium are two of the driving factors for achieving supercontinuum generation. So, supercontinuum generation from a laser source requires an extremely high pulse energy and an extremely short pulse duration. The reader should investigate other sources for more information [14] on the physics of supercontinuum light generation.

2.2 Experimental Setup

Typically for experiments supercontinuum light would be used as part of a chirped white pulse emitter system as introduced in section 1.3.2 where the broad but short pulse would be stretched out in time in a dispersive medium such as a dispersion compensating fiber. The output from the dispersive medium would then be routed to a static test cell for a bench top measurement or an engine for a combustion measurement. More details on experimental setups incorporating supercontinuum light generation will be given in the following chapters.

A few pictures of supercontinuum light are shown in Figures 2.1 and 2.2.

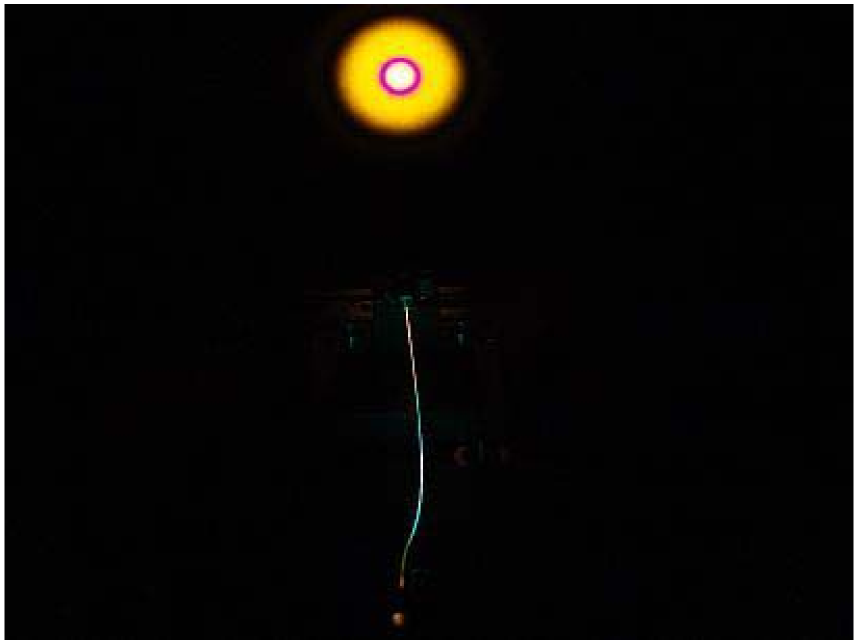

Figure 2.1. Supercontinuum generated in SMF-28 fiber

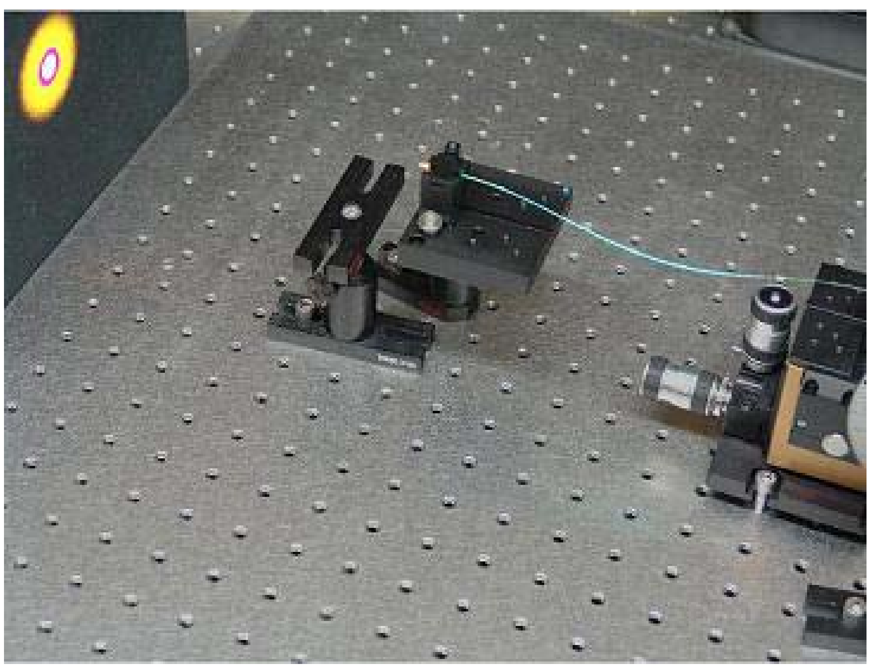

Figure 2.2. Supercontinuum generated in SMF-28 fiber

From the pictures the extremely large bandwidth of supercontinuum light is obvious, especially since the fiber is being pumped with a laser centered at 1557 nm. Blue and green are seen in the fiber and the output from the fiber shows both yellow and red. Assuming a symmetric distribution of colors, this system produced light ranging from ~300 nm to ~ 2700 nm. It is important to remember that given such a wide wavelength spread a large dispersion (i.e. long fiber) would be necessary to make the light useful for measurement and the transmission characteristics of the dispersion medium would most likely limit the bandwidth available for measurement.

2.3 Challenges with Supercontinuum Light Generation

2.3.1 Stability of Source

As both the amplitude and bandwidth of the output light are functions of the laser output, it is absolutely critical to employ a very stable light source. If is necessary to do high-speed measurements, it may also be necessary to employ a mode-locked source to ensure consistency from pulse to pulse.

2.3.2 Fiber Damage

As the bandwidth spread for supercontinuum produced light is a function of the energy density per pulse, it is often desirable to employ a laser that emits a very high amount of energy per pulse. However, extremely high pulse energies have the potential to damage other optical components within a given experimental system, most notably optical fibers. Essentially what happens is that when the pulse energy exceeds the damage threshold for an optical fiber the pulse begins to strip the material off the end of the fiber until the tip of the fiber is sufficiently corroded and damaged. A damaged end to a fiber will output a non-circular, highly speckled light pattern that cannot be efficiently coupled into other fibers.

The important parameters when trying to determine if light will damage a fiber are the pulse duration and irradiance per pulse (energy per area), not the average power of the source measured on something such as a bolometer. For pulse durations longer than 10 ps, the fiber damage pulse irradiance threshold is linearly related to pulse duration. The dominant mechanism for this is essentially excessive thermal heating of the materials and adhesives on the fiber face. For pulse durations shorter than 10 ps, the fiber damage pulse irradiance threshold flattens out (becomes closer to a constant value) and the dominant mechanism for this is the physical stripping of the materials off of the fiber face due to the high pulse energy. More information on this topic is available elsewhere [15], [16].

2.3.3 Broadband Interference

Supercontinuum generated light will largely be subjected to broadband interference that can compromise the signal-to-noise ratio for any reasonably high-speed experimental measurement. Broadband interference will be explained in the next chapter and its propensity to affect supercontinuum light will also be discussed.

2.4 Supercontinuum-based Sensing

Supercontinuum light generation is an extremely valuable technique for generating a broad optical spectrum for spectroscopic sensing of gas properties. As discussed in previous sections, the broadest possible wavelength coverage is desired to be able to record the maximum amount of information about the gas species present in the experiment. Supercontinuum sources lend themselves well to this as this technique can easily result in spectrums with a bandwidth greater than 1000 nm. Also, for spectroscopic measurements an extremely high temporal response is desired along with a high spectral resolution. With a short duration pulsed laser and high-speed detection equipment response times on the picosecond scale are certainly possible. Figure 2.3 is a plot of scan range, scan repetition rate, and spectral resolution for current wavelength scan approaches.

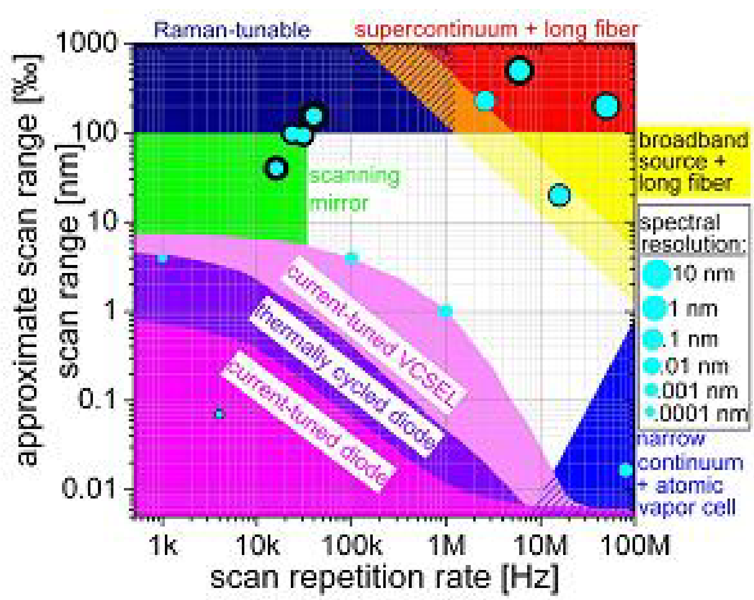

Figure 2.3. Properties of wavelength scan techniques

As seen in the figure supercontinuum generated light dispersed in a long optical fiber provides the largest wavelength scan and the highest scan repetition rate of any of the methods in the diagram. The diagram indicates that supercontinuum light has a rather coarse spectral resolution, but current attempts with supercontinuum light have yielded spectral resolutions as fine as 0.042 nm (see Chapter 4).

2.4.1 Examples of Fiber-based Supercontinuua

Figure 2.4 is a plot of amplitude versus wavelength for supercontinuum light generated in Fujikura dispersion compensating fiber (DCF).

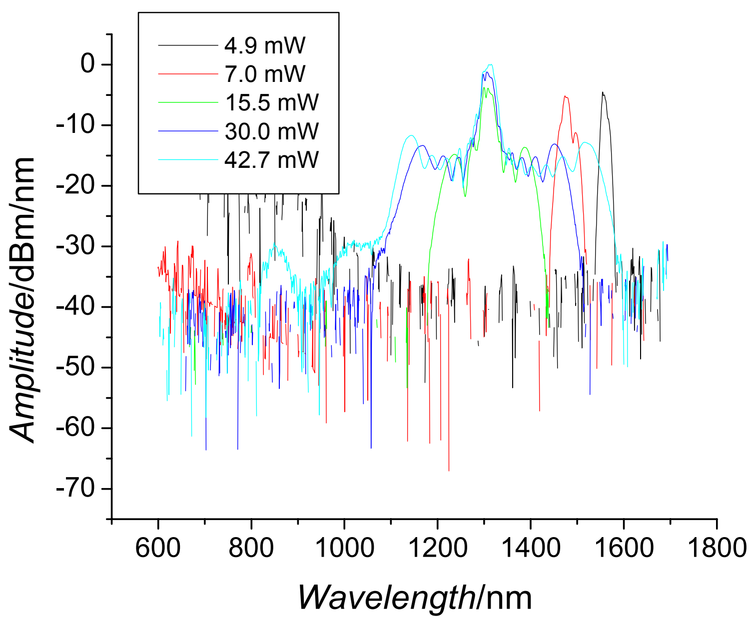

Figure 2.4. Supercontinuum in Fujikura DCF

As seen in the plot increasing the input laser power symmetrically increases the bandwidth of the light (the numbers in the legend are output power from the fiber which corresponds to an increase in laser power). From the graph it is also seen that increasing the power does not cause the amplitude of the plateaus on either side of the pump wavelength to increase but causes the plateaus to further spread. More colors were generated in the Fujikura fiber but are not seen because of substantial fiber attenuation below 1200 nm due to Rayleigh scattering and above 1700 nm due to silica absorption (the prime material in optical fiber). In fact, light was generated all the way through the visible end of the spectrum as blue light was seen at the entry tip of the Fujikura fiber.

One very interesting effect from generating supercontinuum in this fiber that cannot be explained at this time is the blue shift in pump wavelength (initially centered at 1557 nm). This was not seen when using any other kind of fiber and theories for this will hopefully be tested in the future in search of an explanation for this phenomenon.

Figure 2.5 is a plot of amplitude versus wavelength for supercontinuum generation in Metrocor optical fiber.

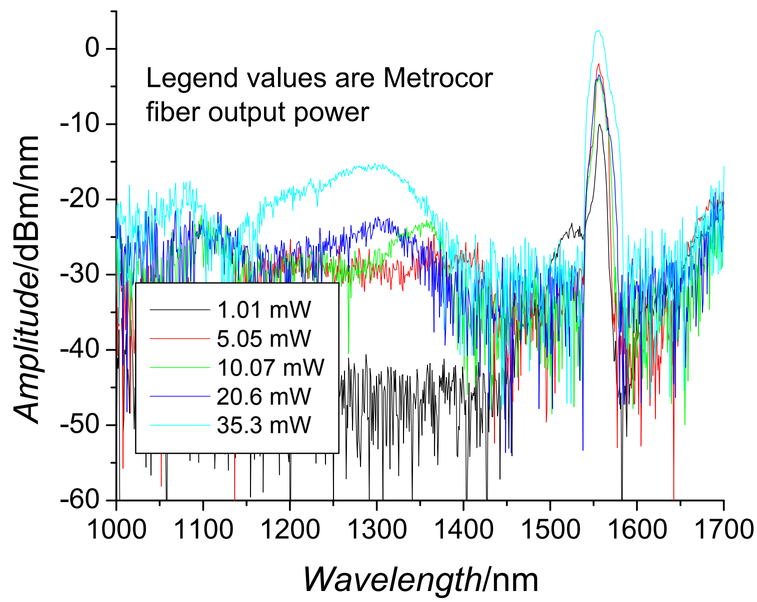

Figure 2.5. Supercontinuum in Metrocor fiber

As with the Fujikura fiber, increasing the laser power causes the bandwidth of the light to increase. The spectrum extends farther into the red wavelengths but unfortunately the optical spectrum analyzer that was used to monitor this signal only allowed measurement up to 1700 nm. Metrocor fiber does not generate supercontinuum light as well as the Fujikura DCF, but it does show significant growth away from the pump wavelength.

2.4.2 Absorption Measured with Supercontinuum Light

The broadband capabilities of supercontinuum generated light are nicely illustrated in Figure 2.6.

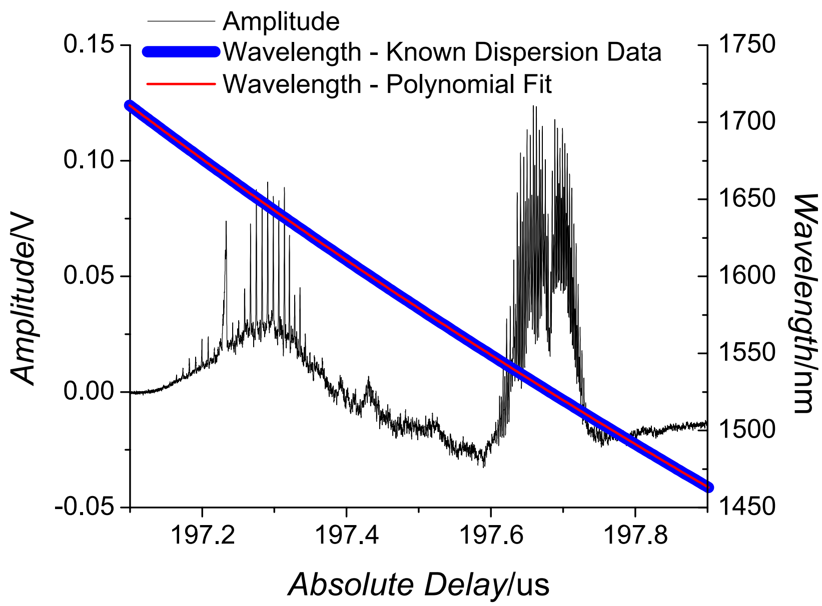

Figure 2.6. Methane and acetylene absorption lines in supercontinuum generated light

Methane absorption lines are seen on the left and acetylene absorption lines are seen on the right. For this test photonic crystal fiber (PCF) was used for supercontinuum generation. This data was taken on a high-speed oscilloscope as amplitude versus time and a wavelength axis was fitted in post-processing by using known dispersion data to fit a polynomial to the recorded time. From the plot it is seen that a wavelength spread of 300 nm was used to measure two separate species in a time of 1 μs. This should serve as a reasonable example of the possibilities for measurements utilizing supercontinuum light generation. This technique has some exciting possibilities and much progress is anticipated for the near future.

CHAPTER 3 – BROADBAND INTERFERENCE

3.1 Interference Background

Interference occurs when multiple colors of light overlap in space and interfere with each other. As the individual colors are not of the exact same wavelength, their phase varies at different locations and the interference they are causing thus varies in time. Therefore, the interference that is seen by a detector depends on the time at which it was detected. Interference introduces a time-dependent variation of the light intensity. For example, this can lead to fluctuations when the power of a polychromatic continuous wave is detected. Obviously, the induced variations also compromise time-of-flight spectroscopy. Time variations due to broadband interference may mask or even mimic spectral features such as absorption lines of absorbers in the light path. The two main issues here are the time dynamics and the pulse-to-pulse stability of the variation. If the time dynamics and the amplitude of the interference are the same as or faster/greater than that of a spectral feature occurring in the time trace, the latter gets obscured. Interference degrades pulse-to-pulse stability, and without stability measurements taken on a singleshot basis (without digital averaging) will have significant error and a lot of times will be useless for data analysis. Detailed information on the underlying physics of interference due to the presence of broadband light is available and the reader is encouraged to look elsewhere for more information [17].

3.2 Issues with Broadband Light Sources

As referenced to earlier, it is often advantageous when making spectroscopic measurements to use a source that has the broadest wavelength span possible to monitor the maximum amount of information about the system of interest. However, any system that employs a broadband light source will inherently have some degree of interference. Often times, the interference is not seen because the time response of the detection system is too slow or the data is taken with multiple averages which essentially also slows the detection response time. For example, an optical spectrum analyzer (OSA) recording absorption of a static environment would not see broadband interference because it has a very slow response time and the interference would essentially average itself it out before the OSA would notice anything. Also, even if using a high-speed detector and oscilloscope to record absorption data interference effects would be washed out if the data was averaged 1000 times before being displayed and recorded.

Even though broadband interference might not appear directly in measurement data, interference is always present and its presence should at least be acknowledged when making optical measurements.

3.3 Distinction Between High and Low Quality Light

The large majority of light from a broadband source suffers from interference effects and yields what can be termed low quality light. However, a small portion of the light from a broadband source may not be subject to interference and therefore can be viewed as high quality light.

When light travels through something such as an optical fiber, its propagation speed is the speed of light divided by the index of refraction. The index of refraction has a small wavelength dependence so the different wavelengths travel at slightly different speeds through the fiber. In typical optical fibers, higher wavelengths ("red") have a slightly lower index of refraction than smaller wavelengths ("blue") so the red wavelengths travel faster than the blue wavelengths. So, in a fiber higher wavelengths will slowly pass by lower wavelengths as the light propagates through the fiber. This is why interference has a spatial dependence and will be different at each location in a fiber. As most broadband sources produce light with a bell-shaped spectral distribution, most of the source output will see other colors as it propagates through a fiber and will be subject to broadband interference. However, a small portion of light at the far ends of a source's spectral distribution will travel either fast or slow enough such that it will not be affected by the presence of other colors. This light therefore will not have any interference issues and is what shall be referred to as high quality light. Figure 3.1 illustrates this idea of high and low quality light.

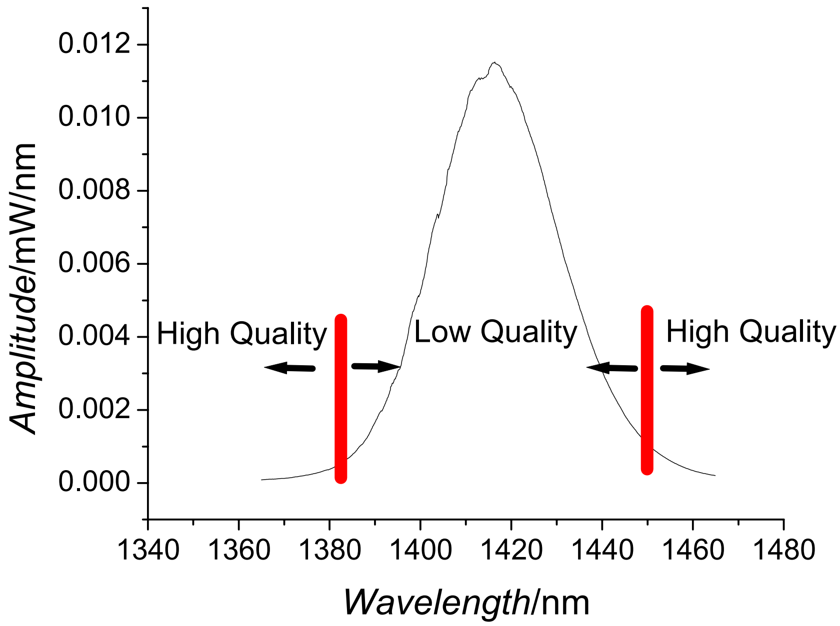

Figure 3.1. High and low quality light diagram

As seen in the diagram the majority of the light, especially for a source with a gaussian-shaped distribution such as this, falls into the category of being low quality. The lines drawn as the dividing points between high and low quality are just estimations, but they do show the unfortunate consequence that most light from a broadband source is low quality.

High quality light is often times preferable because with a stable light source it will be seen as steady and non-varying and can be used to make singleshot (non-averaged) measurements. On the other hand low quality light, even with the most stable, rock-solid laser source in the world, still will often times produce signals that need to be heavily averaged or require other means to deal with interference problems. So, high quality light appeals because it can be used to make high-speed measurements without having to make any compromises or require other additions to the experimental system.

Unfortunately, as explained previously, most light from a broad source will be low quality and this limits the bandwidth of high quality light. Also, as only the edges of a source's distribution will be high quality the high quality light will typically have significantly lower power than the low quality light. So, high quality light has its advantages but is not the perfect solution because most light from optical sources is low quality which limits the utility of making measurements with high quality light. Using each type of light for making absorption measurements will be chronicled later in this paper and the reader can make their own judgments on the pros and cons of both methods.

3.4 Methods to Deal with Broadband Interference / Low Quality Light

There are methods to deal with broadband interference present in low quality light such that acceptable laboratory measurements can be made. Choosing the best way to go about this is dependant on what specifications are necessary for the measured data, what equipment is already available in a laboratory, and what additional equipment is affordable for purchase if necessary.

3.4.1 Extremely Short Pulse Duration / Increased Dispersion

This approach mitigates interference issues by slowing down the time dynamics, or beat frequency, of the interference. In order to easily distinguish a spectral feature against variations due to interference, the dynamics of the interference have to be slower than that of the features. If the time dynamics of the interference are faster than that of the spectral features, the spectral features become hard to discern and will have significant error. According to [17], the beat frequency in time-of-flight spectroscopy (TOFS) is determined by the ratio of dispersion and pulse length:

$$f_{beat} = \frac{c\Delta t_{pulse}}{\lambda^2 \, |D|},$$

Equation 3.1. Beat frequency for TOFS

where f_{beat} is the beat frequency, *c* is the vacuum velocity of light, Δt_{pulse} is the pulse duration, λ is the wavelength of the light, and $|D|$ is the absolute value of the dispersion. As seen in Equation 3.1, decreasing the pulse duration and/or increasing the dispersion both decrease the beat frequency of the interference. In other words, short duration pulses and/or a high dispersion enhance the discrimination of interference and spectral features. To elucidate this approach the following example is introduced. For this case, say a typical spectral line width of 0.1 cm^{-1} at 1530 nm [10] is to be investigated. The dispersion present in the system is that of a commercially available dispersion fiber, which for an acceptable level of attenuation typically is -3 ns/nm or higher. For this dispersion the spectral feature appears as a modulation in the chirped pulse, and the duration of the modulation is about 70 ps. In order to make this feature distinguishable the beat frequency has to be smaller than 1/(70 ps) = 14 GHz. According to Equation 3.1 a pulse of 300 ps or shorter fulfills this condition. This example clearly demonstrates the feasibility of this approach with common technologies such as picosecond and femtosecond lasers. This is nicely illustrated in Figure 3.2.

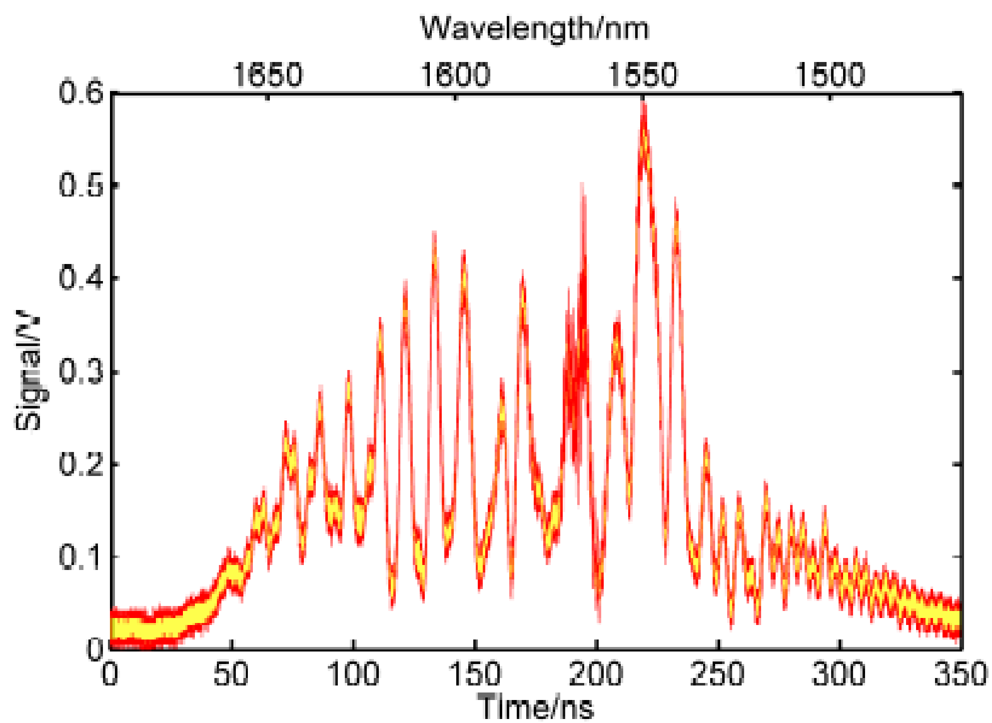

Figure 3.2. Slowing of interference beat frequency to combat broadband interference

To produce this plot, a pulse from a laser with a pulse duration of 150 fs was captured using a high-speed photoreceiver and oscilloscope. The sawtooth pattern shown in the figure is broadband interference. Even though the interference was very strong for this measurement, it is discernable and was very stable so this signal could still be used to make absorption measurements.

One main concern with this approach is that although the modulation of the optical power is slower than that of the spectral features, the interference can cause the minimum power to be significantly lower than the average power, which could result in an unacceptable signal-to-noise ratio at some points on the measured spectrum. This is also seen in Figure 3.2. Another issue with this approach is related to the dispersion medium. When a dispersion fiber is utilized for TOFS a higher dispersion increases the attenuation of the light transmitted through the fiber. While the dispersion increases linearly with fiber length, the attenuation increases exponentially with length as typical fiber attenuations are rated in dB/km (decibels per kilometer). So, reducing broadband interference also reduces the power available at the detector with this approach.

Another issue that needs to be addressed in conjunction with the time dynamics of the interference is the ability to fit a baseline curve (I_o) to an absorption spectrum (I). Unless the baseline curve is measured separately, this step is necessary to be able to determine the absorption. If there is no interference present in the system, it is very easy to resolve the initial light spectrum from the absorption spectrum as was shown in Figure 1.6. However, if there is interference it becomes increasingly more difficult to get an accurate representation of the baseline curve as the time dynamics of the interference increase. So, once again it is desirable to have the time dynamics of the interference as slow as possible when compared to the actual absorption spectrum.

3.4.2 Increased Coherence Length

The thrust behind employing a light source with a sufficiently large coherence length is not to eliminate broadband interference, but rather to insure an extremely stable interference pattern from pulse to pulse. If the coherence length of the light is larger than the spacing between two adjacent pulses, the interference pattern on the time-dispersed signal will occur at the same time within the light pulse. This feature could be exploited as follows. If the spectral signature to be detected stems from an absorption line, the time-dispersed light could first be directed through the experiment containing the absorber, and then a pulse could be detected without any absorbers present. This constitutes a straight forward means to acquire spectra of the attenuated and the un-attenuated light. These reference spectra could then be analyzed by applying Beer's law. As with the short pulse/high dispersion method, the stable interference resulting from this approach still has the potential to produce an unacceptable signal-to-noise ratio at the points of maximum destructive interference.

Another way to insure a stable pulse would be to use multiple averages when recording the signal. However, this is often times undesirable as the time resolution of a measurement suffers when averaging is employed as was mentioned previously. This approach might be satisfactory for some applications but is an unacceptable compromise for applications requiring ultra-short detection times.

The setup for this method is no different than that of a typical time-of-flight spectroscopy setup except that a light source with a large coherence length would be employed. Candidates for light sources include mode-locked picosecond and femtosecond lasers. Other light sources such as LEDs and ASEs, in which the light generation is based on random, spontaneous emission processes, are not suitable for this approach.

3.4.3 Split Pulse

In cases where the modulation due to interference masks spectral features and in which the interference is not stable from pulse to pulse a means of single-pulse referencing allows the spectral features to be inferred from the recorded signal in a fashion similar to that in Section 3.4.2. The method behind this approach is to split the light, run a portion of the light through a delay line, and then recombine the two and detect them with a single photoreceiver. One part of the light would be directed through the measurement region and the other would be directly relayed to the aforementioned detector. By using only one detection system for both light pulses it is ensured that distortions and noise are affecting them both in a similar manner. Since the reference signal is available, it is possible to identify the spectral features in the signal even if the interference occurs on the same time scale as the feature. It is assumed that the same interference will appear in each portion of the split pulse as both originated from the same initial pulse but will have no correlation or resemblance to the interference in split pulses from different initial pulses. The non-correlation is due to the short coherence length of the light. For this approach it is assumed that there is no noticeable difference in the dispersion in the two detection arms. More detailed information on the split pulse approach to counteract interact can be found elsewhere [18].

Figure 3.3 shows a schematic of a basic system employing the split pulse approach.

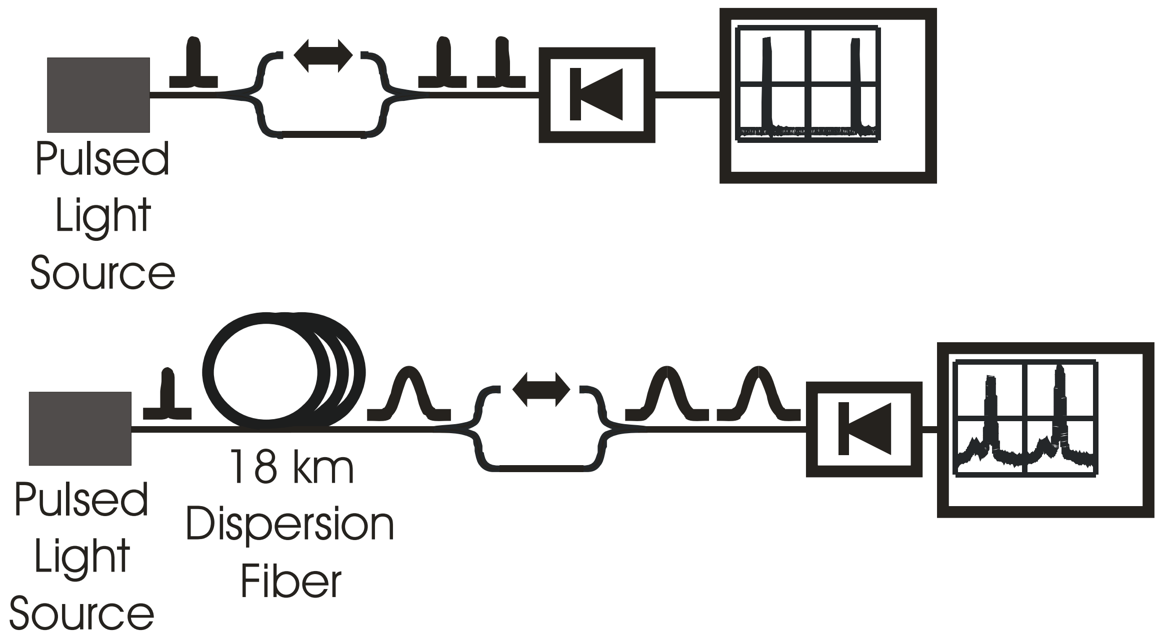

Figure 3.3. Split pulse setup with and without dispersion

The difference between the two schematics is that the bottom one incorporates dispersion. As seen in the figure, one part of the split light goes through some kind of delay and ends up behind the other part. Both parts are collected into the same detector and read into the same oscilloscope. When employing this approach, care must be taken such that the oscilloscope is sampling the exact same points for each of the two pulses. Even with an oscilloscope capable of sampling at 50 ps/pt or faster it is still possible to have a large amount of error due to each of the two pulses being digitized differently. If possible, it is a good idea to incorporate variable length into one of the paths so that adjustments can be made to ensure that the same points on both pulses are being sampled. If it is not possible to adjust the path lengths such that the same points are being digitized, it is possibly to resample the data by adding more points between the recorded points and interpolating the resampled data. This helps but if at all possible it is best to incorporate some level of variable length into one of the paths for this method.

Once data has been taken, it must be post-processed to cut the data so the two pulses can be divided and the absorption can be calculated from the quotient as described in Beer's Law. Results from an experiment to show the viability of the split pulse method are shown in Figure 3.4.

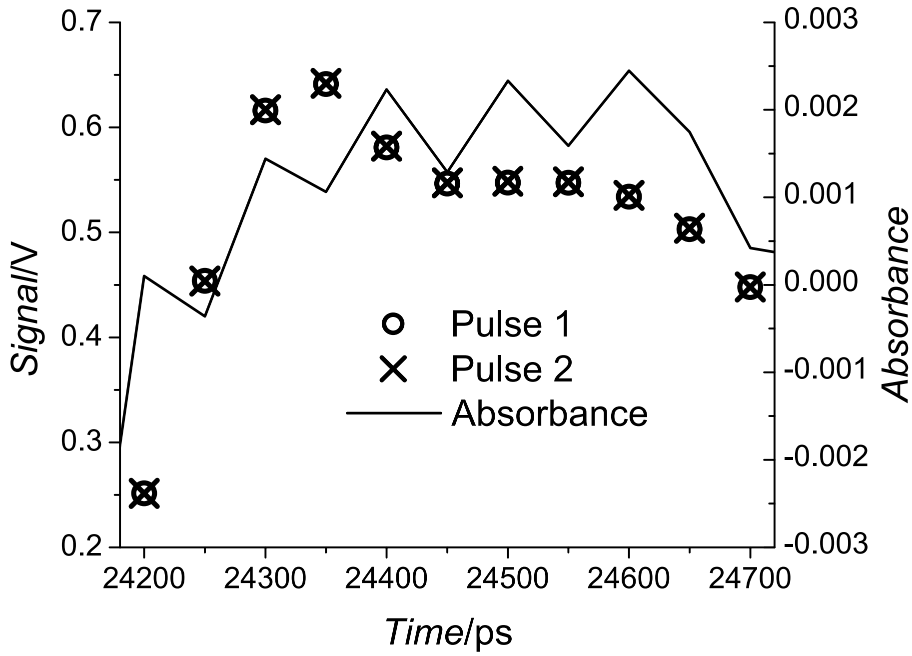

Figure 3.4. Split pulse approach results

From the figure the x's and o's correspond to the points that were recorded for each of the two pulses and correspond to the signal axis on the left. The length of the one of the paths was adjusted so that the detector was recording the same points in space and time for each of the pulses. This is illustrated nicely in the plot as the x's and o's fall right on top of each other. The absorbance is calculated for each set of points and this corresponds to the vertical axis on the right. As there was no gas being measured, the results from this test show an absorbance error of approximately 0.1% as any non-zero absorbance for a test such as this is in error.

CHAPTER 4 – EXPERIMENTAL EQUIPMENT SPECIFICATIONS

4.1 Laser Specifications

The laser used for the CO measurements covered in this paper (Chapters 5 and 6) was an IMRA B-250 erbium doped fiber laser manufactured by Aisin Seiki Co. Ltd. The laser has a pulse energy of 1.5 μJ/pulse, a 200 kHz repetition rate, and a pulse duration of 900 fs. This results in a peak power of 1.6 MW and a duty cycle of 0.00002%. The laser operates at these specifications all the time when switched on and cannot be varied.

4.2 Gas Cell Specifications

The gas cell used was a cylindrical aluminum cell 2 m in length and 50 mm in diameter. The cell had AR coated wedged glass windows on both ends to provide optical access to the contents of the cell. A laboratory gas bottle filled with CO was plumbed into one side of the cell and a vented exhausted was plumbed to the other side. Both the CO inlet and exhaust outlet had ball valves which allowed the cell to be filled and then closed so that the cell contents were essentially stagnant while measurements were taken.

4.3 Optical Fiber Specifications

SMF-28 fiber is standard telecommunications fiber that has silica as its main constituent and has a core diameter of 9 μm. SMF-28 has maximum transmission at approximately 1550 nm with Rayleigh scattering (inversely proportional to λ^4)

attenuating light at lower wavelengths and the silica material absorbing light at higher wavelengths. A plot of typical SMF-28 attenuation is shown in Figure 4.1 (attenuation is the opposite of transmission).

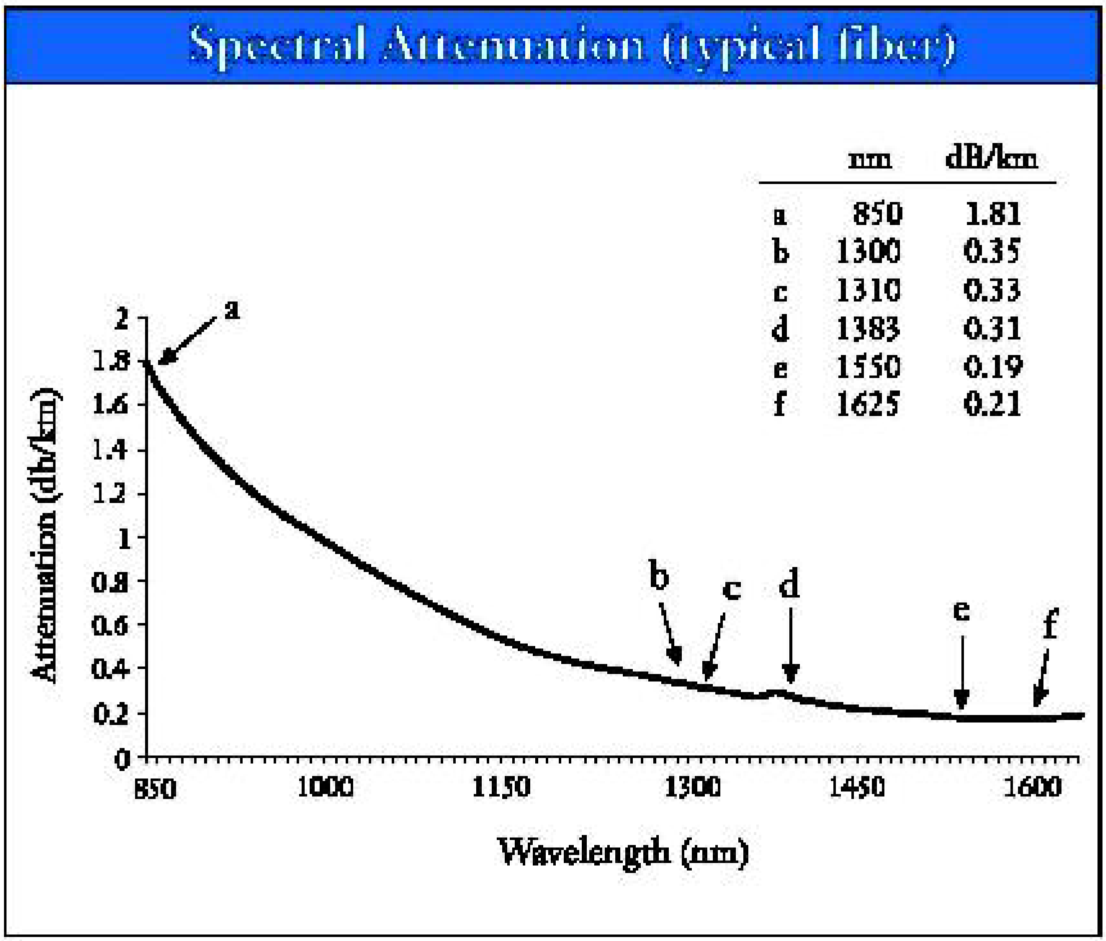

Figure 4.1. Typical fiber attenuation

GR multimode fiber also has silica as its main constituent but it has a larger core diameter of 62.5 μm. Its transmission characteristics are similar to that of SMF-28 fiber and what is shown in Figure 4.1.

The fiber that was used for supercontinuum generation was an OFS RightWave WBDK-43 Dispersion Compensating Module (DCM). This fiber has an effective diameter of 5.2 μm, a length of 500 m, and a dispersion of -49 ps/nm at 1550 nm.

The dispersion fiber used for these experiments was a Fujikura Dispersion Compensating Fiber (DCF) 40 km in length with an effective diameter of 6 μm and a dispersion of -4012 ps/nm at 1400 nm.

It should be pointed out that negative dispersion for a fiber means that longer wavelengths travel faster than smaller wavelengths and for positive dispersion the opposite is true.

4.4 Fiber Splitter Specifications

The fiber splitter used for these experiments was a Fiber Instrument Sales manufactured FIS Dual Window 1310/1550nm 2X2 Coupler with a 50% / 50% split ratio between the two output legs of the splitter.

4.5 Beamsplitter Cube Specifications

The beamsplitter cube used for the experiments discussed in Chapters 5 and 6 was a Thorlabs 1100 – 1600 nm broadband beamsplitter cube. The cube dimensions are 10 mm X 10 mm X 10 mm.

4.6 Photoreceiver Specifications

The photoreceiver used to measure absorption in the CO-filled cell described in upcoming chapters was a New Focus Model 1592 DC-coupled 3.5 GHz InGaAs IR photoreceiver. The photoreceiver used to detect the optical trigger pulse from the IMRA laser was a New Focus Model 1544 AC-coupled 12 GHz near-IR photoreceiver. Both photoreceivers were powered by a New Focus +/- 15 V current limited power supply.

4.7 Oscilloscope Specifications

The oscilloscope used for these measurements was a Tektronix TDS 7404 Digital Phosphor Oscilloscope. This oscilloscope has four inputs that can either be for BMC or SMA connectors. The maximum digitization resolution for this scope is 50 ps/pt and the response rate is 4 GHz.

4.8 System Response Time and Spectral Resolution

The response time for an optically-based experimental system such as the one used to take data for this paper is a function of the laser pulse duration, the detector response rate, and the oscilloscope response rate. The laser pulse as stated previously is 900 fs, so the laser response time is simply:

$$\tau_{laser} = 900 \times 10^{-15} s$$

Equation 4.1. Laser response time

To calculate the detector and oscilloscope time responses (s) from their respective response rates (Hz), the relevant formula is:

$$\tau = \frac{0.44}{f[Hz]}$$

Equation 4.2. Formula relating response time and response frequency

where the 0.44 constant comes from the assumption that the optical beam profile is Gaussian, which is generally an accurate assumption.

So,

$$\tau_{\det ector} = \frac{0.44}{3.5 \times 10^{9}\, Hz} = 1.26 \times 10^{-10}\, s$$

Equation 4.3. Detector response time

and

$$\tau_{oscilloscope} = \frac{0.44}{4 \times 10^{9}\, Hz} = 1.1 \times 10^{-10}\, s$$

Equation 4.4. Oscilloscope response time

The net response time for the system is then the square root of the sum of the squares of the individual response times. So,

$$\tau_{net} = \sqrt{\tau_{laser}^2 + \tau_{\det ector}^2 + \tau_{oscilloscope}^2} = 1.67 \times 10^{-10}\, s = 167\, ps$$

Equation 4.5. Net response time for experimental system

The response time for the optical system used for the experiments conducted in chapters 5 and 6 had a response time orders of magnitude smaller than those of the typical mechanical equipment described in Chapter 1 (a type K thermocouple had a response time as small as 0.25 seconds and an engine capable pressure transducer had a time constant of approximately 0.1 seconds). The advantage of employing optical methods should be obvious from this comparison alone.

The spectral resolution for an optical system is simply the laser pulse duration divided by the net dispersion of the system. The laser pulse duration as stated previously is 900 fs, and the dispersion of the Fujikura DCF dominates everything else in the system so only it will be considered (SMF-28 fiber actually has a small positive dispersion which will be assumed to essentially cancel the small negative dispersion from the OFS DCM used to generate supercontinuum). The spectral resolution is then:

$$R = \frac{167\,ps}{4012\,\frac{ps}{nm}} = 0.042nm$$

Equation 4.6. Spectral resolution for experimental system

To compare, this calculated resolution of 0.042 nm for the experimental system described in this paper is smaller than both estimates of a typical combustion spectral linewidth (0.06 nm and 0.18 nm). So, this system should be able to sufficiently track all absorption lines occurring in this experiment as well as for any optical experiment.

CHAPTER 5 – Carbon Monoxide (CO) HIGH QUALITY LIGHT MEASUREMENTS

5.1 Requirements for High Quality Light Measurements

As discussed in Section 3.3, there is a very important difference between high and low quality light. High quality light is largely free of interference issues and can be used in a relatively straightforward manner for making optical measurements while low quality light is stricken with often times severe interference. Averaging or more complicated (possibly more expensive) means must then be used in order to make reasonable measurements with low quality light. Within a broad spectrum, high quality light constitutes the edges of the spectrum because this light travels either fast enough or slow enough such that it does not interact and interfere with the other wavelengths.

Where light transitions from high quality to low quality and vice versa is not exactly a well-defined point and is somewhat dependant on the application and the accuracy and time response requirements for a given experiment. A good yardstick for determining where light may be high quality is to look at the collected light spectrum on the detection equipment of choice and determine the stability of the signal. High quality light should be stable on a singleshot basis or with minimal averaging. Anything that requires significant averaging (i.e. 100 averages or more) would have to be considered low quality and means to lessen the effects of interference or deal with the interference as is should be investigated.

5.2 Experimental System Schematic

The experimental system that was used to produce high quality light and use it to make CO absorption measurements is shown below in Figure 5.1.

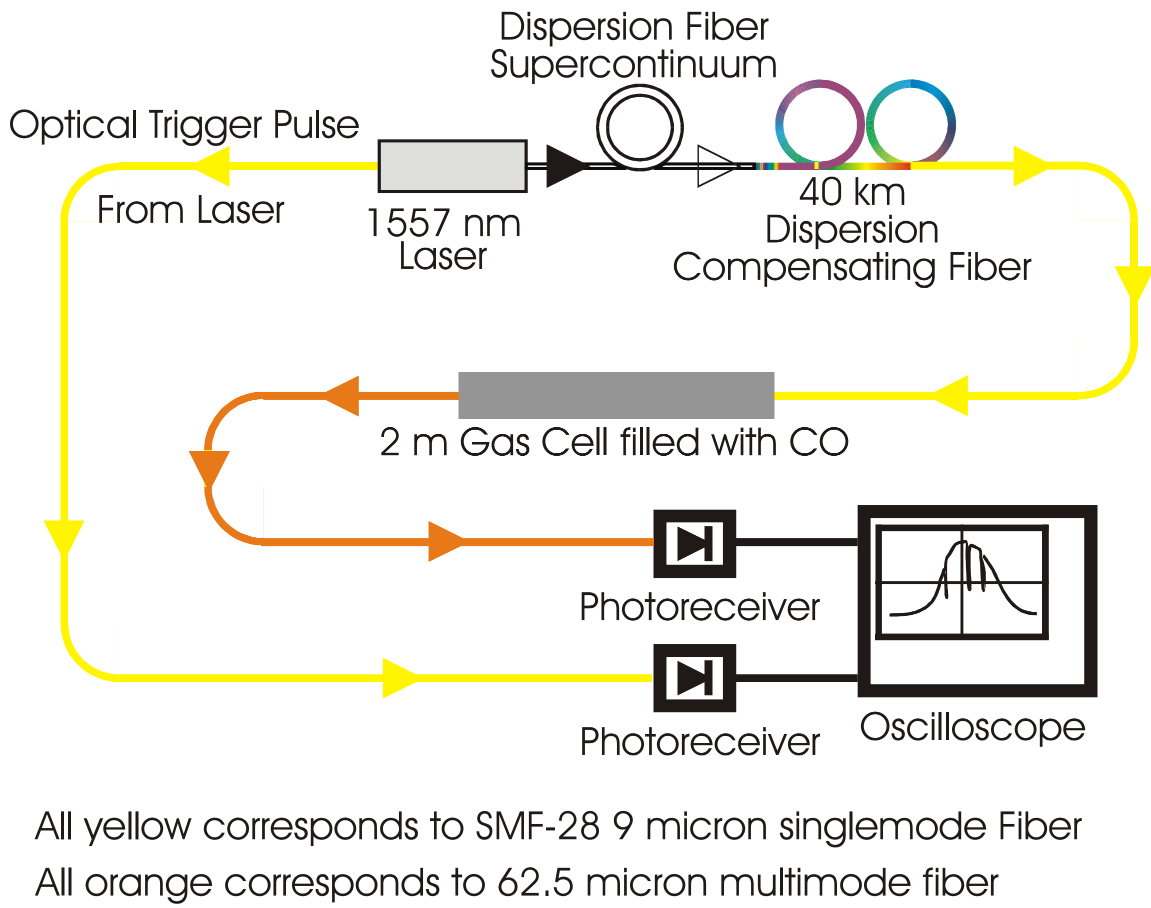

Figure 5.1. Experimental system for high quality light CO absorption measurements

Narrow bandwidth light centered at 1557 nm was output from the IMRA laser and coupled into OFS dispersion fiber to induce supercontinuum generation. The supercontinuum generation produced a short duration, extremely broad white pulse that was routed into 40 km of dispersion compensating fiber (DCF). In the DCF, the white light stretched out in time and space to form a pulse with a wavelength resolution of 0.042 nm. This stretched pulse was sent through a short length of SMF-28 singlemode fiber and then directed as light in free space through a 2 m gas cell filled with CO at approximately 25 psi. The free space light upon exiting the cell was coupled into 62.5 graded index (GR) fiber using a lens and precision stage. The light collected in the GR fiber was routed to a high speed photoreceiver and high-speed digital oscilloscope for display. An optical trigger pulse from the IMRA laser was used as a trigger for the digital oscilloscope and this was read on another high-speed photoreceiver. Due to the essentially zero amount of CO in atmospheric room air no purging was required for this system.

5.3 Data and Results

The spectrum that was used to make high quality light CO absorption measurements is shown in Figure 5.2.

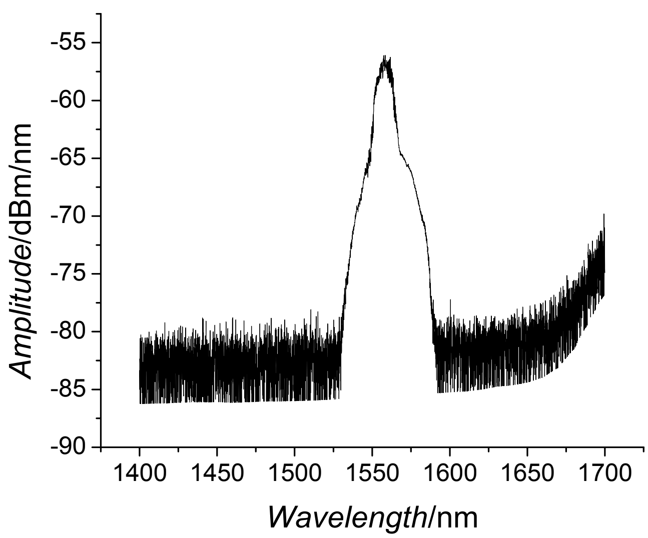

Figure 5.2. Spectrum for high quality light CO absorption measurements

From the spectrum it is seen that the spectrum is centered at approximately 1557 nm and is relatively narrow when compared to supercontinuum generation and other means of achieving broadband light. The input power to the supercontinuum fiber was kept low enough such that no supercontinuum generation occurred by employing a variable, wavelength-independent optical filter. This was done because CO absorbs light between 1560 and 1600 nm and it was desired for this case to have the red end of the spectrum from this laser just extend into the CO absorption band to ensure high quality light for taking measurements.

Figure 5.3 shows the full data trace that was taken on an oscilloscope after being sent through the CO-filled cell.

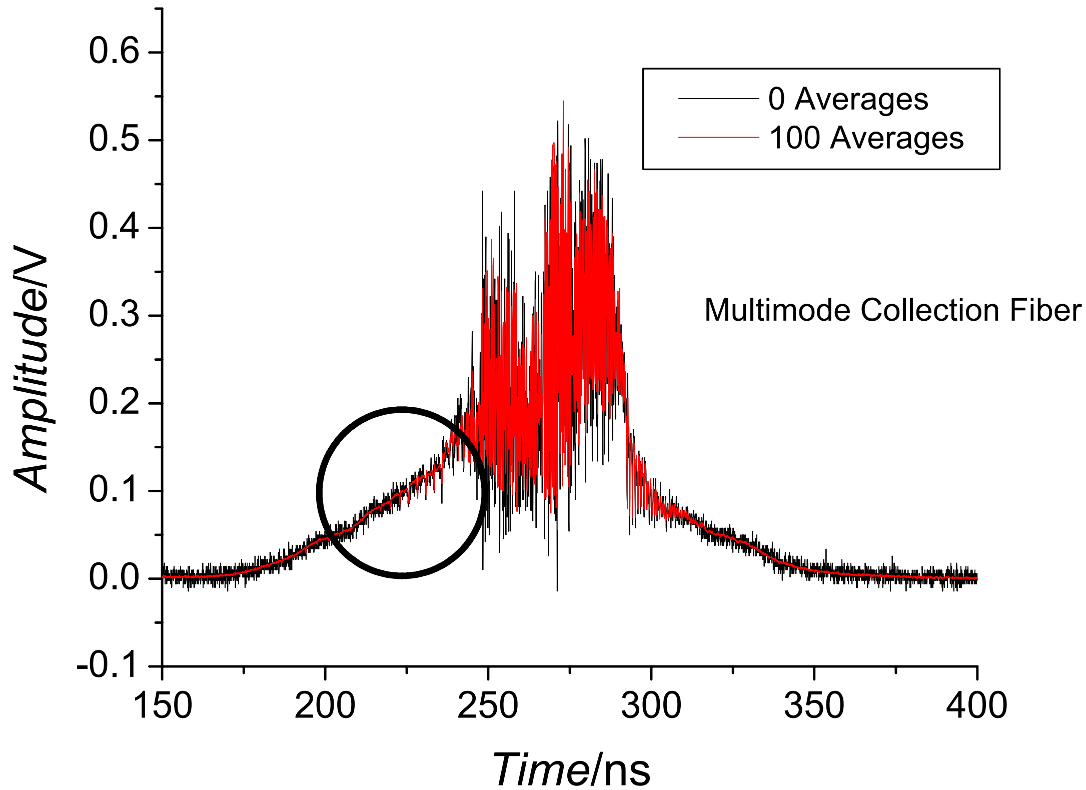

Figure 5.3. Complete time trace of high quality light CO measurements

The difference between low and high quality light is very evident in this figure. The large share of the light collected in the center of the trace has a signal-to-noise ratio of approximately 1 to 1 and is most definitely low quality light that has been subjected to strong broadband interference. With such a low signal-to-noise ratio, any high speed measurements (i.e. little or no averaging) are not possible in this regime without other means to counteract interference issues.

Looking at the circled area on the left side of the trace, high quality light is seen. Broadband optical interference is not present in this part of the recorded spectrum and the noise that is seen is detector noise in the photoreceiver and digitization noise in the oscilloscope, both of which are inherent when using the necessary equipment for this measurement. Figure 5.4 is a trace of the circled region shown in Figure 5.3 with the oscilloscope zoomed in on the high quality light region only.

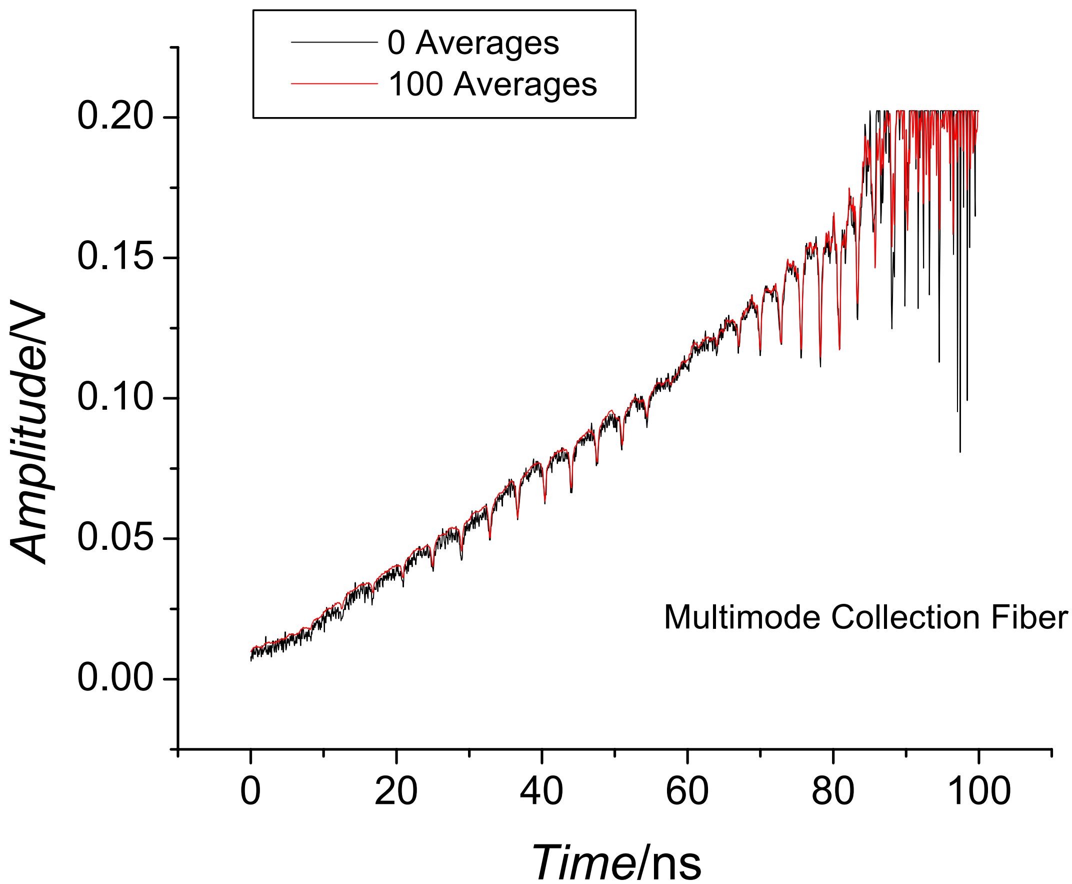

Figure 5.4. High quality light CO absorption lines

From the plot several CO absorption lines are seen for both the singleshot and 100 average measurements. The absorption lines are much stronger than the signal noise, and the resulting absorption error for the singleshot case is approximately 3% with the 100 average case being even better. This is very good for a singleshot high-speed measurement, especially since the shot noise limit for this data was estimated to be 1%. With such low noise, it is possible to pick out the center of the CO absorption band which occurs at approximately 1575 nm and corresponds to approximately 60 μs on the time axis. As the dispersion fiber used for this experiment has negative dispersion, the P branch of the CO absorption spectrum arrives at the detector first and is seen before 60 μs while the R branch of the spectrum arrives later and is seen after 60 μs.

For this measurement, approximately 40 nm of light was available on one side of the overall light spectrum as high quality light for making high speed measurements. As it was desired to measure CO, care was taken such that this 40 nm on one side of the spectrum appeared in the CO absorption band. As the light spectrum was roughly symmetric, it is estimated that another 40 nm or so of light was available on the other side of the spectrum for making high quality measurements but for this experiment nothing was done to utilize this.

CHAPTER 6 – Carbon Monoxide (CO) LOW QUALITY LIGHT MEASUREMENTS

6.1 Requirements for Low Quality Light Measurements

As one would expect, having low quality light available for a measurement is much easier to achieve than high quality light. In fact, all that is required is to have sufficient optical power in the wavelength range of interest. It is of course convenient to have a stable light source but this is not as critical for making low quality light measurements.

There are essentially two schools of thought on ways to counteract the interference that plagues low quality light: a lot of digital averaging or one of the methods described in Section 3.4 of this paper. Averaging of course is very easy to employ with a digital oscilloscope but this greatly slows down the time response for the detection system as the time response is inversely proportional to the number of averages. For non-transient measurements this would be okay but for anything that is dynamic in nature this would probably not be acceptable. For experimental means to deal with interference, the split pulse approach as diagrammed in Section 3.4.3 was used and the results from this will be described in this chapter. The other methods listed in Chapter 3 certainly were feasible for this experiment but were not employed in the laboratory.

6.2 Experimental System Schematic

A schematic of the experimental setup that was used for making low quality light CO absorption measurements is shown below in Figure 6.1.

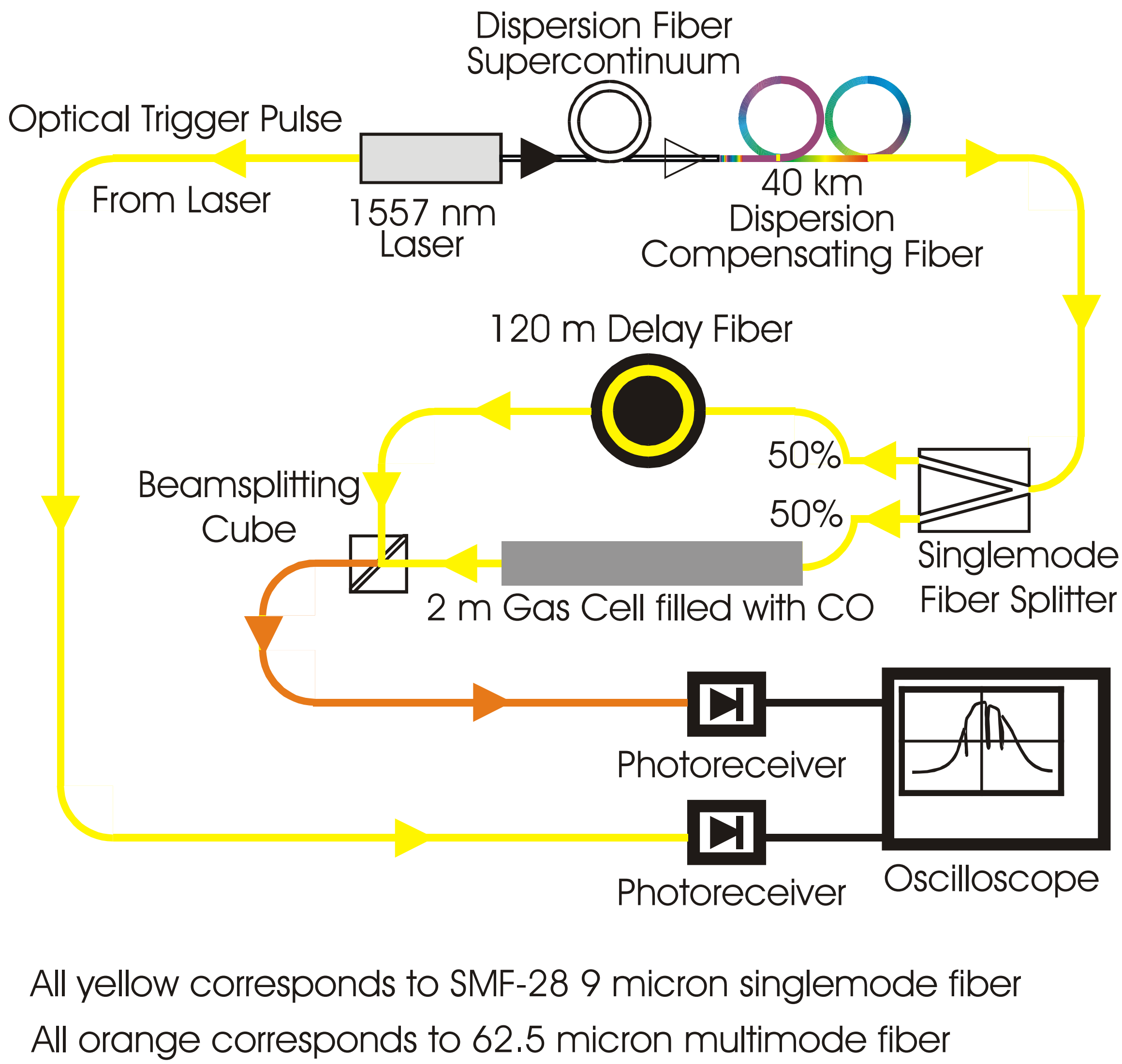

Figure 6.1. Experimental system for low quality light CO absorption measurements

This setup is very similar to the system used for the high quality light measurements discussed in Chapter 5 except for a few key differences. Light was taken from the same laser but this time the input power to the OFS fiber was high enough such that supercontinuum generation occurred. After exiting the supercontinuum fiber the light was split using a singlemode fiber splitter. 50% of the split light was directed through the CO-filled cell and the other 50% of the light from the splitter was ran through a 120 m SMF-28 fiber that served to delay this part of the pulse so it would arrive at the detector behind the pulse that was shot through the CO cell. Both parts of the initial pulse were directed at a beam-splitting cube which served to direct both pulses at a lens which coupled all of the light back into either a singlemode or multimode collection fiber. The collection fiber was directed to the same photoreceiver and oscilloscope as was used for the high quality light measurements presented in Chapter 5. The same trigger pulse setup was also used.

A photograph of the laboratory setup for this measurement is shown in Figure 6.2.

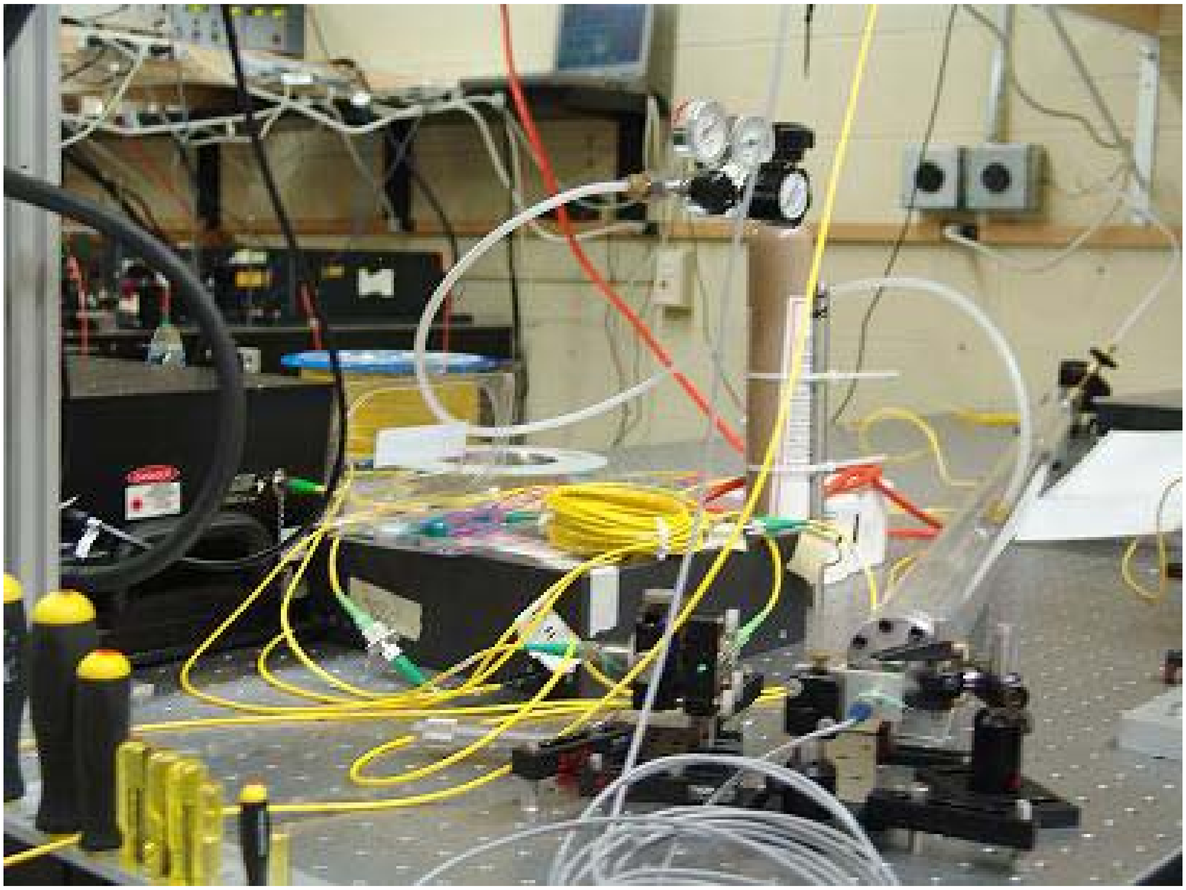

Figure 6.2. Laboratory setup for low quality light CO measurements

On the far left the laser is visible and the box in the middle of the picture contains the 40 km dispersion fiber. The gas cell filled with CO is on the right of the photograph and the brown CO bottle is standing vertically towards the center of the picture. The supercontinuum fiber is on the gray spool towards the back of the picture and several yellow SMF-28 fibers are visible throughout along with a gray multimode fiber that was used for collecting the light after the gas cell. A zoomed in shot of the beamsplitter cube and collection fiber are shown below in Figure 6.3.

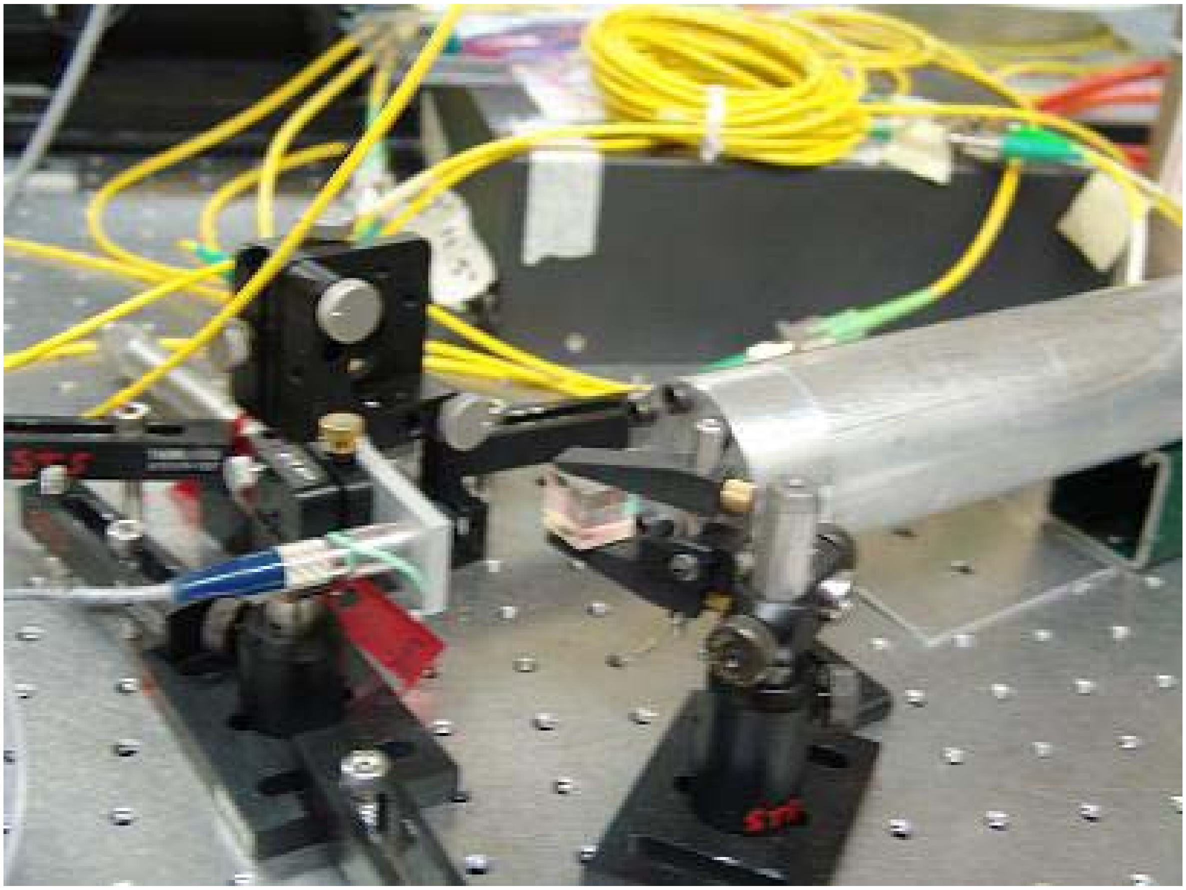

Figure 6.3. Beamsplitter cube used to couple both parts of optical pulse

The cube is easily seen in the picture, the gas cell is on the right, the second half of the split light pulse is towards the upper left, and the multimode collection fiber is on the left of the photograph. Incorporating the split pulse approach makes the laboratory setup more difficult when measuring with low quality light as compared to high quality light but not impossible.

6.3 Data and Results

The light spectrum that was used for making low quality light measurements of CO absorption is shown in Figure 6.4

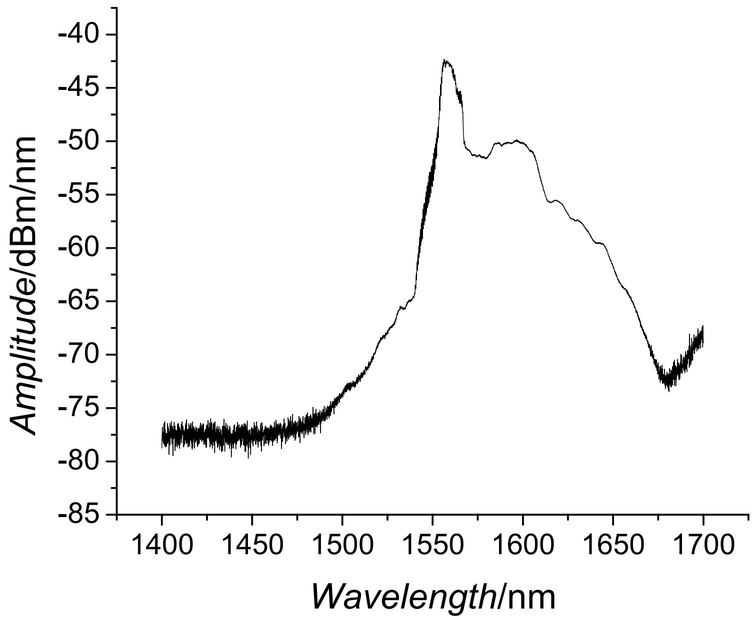

Figure 6.4. Low quality light spectrum for CO absorption measurements

The spectral peak occurred at 1557 nm and was the pump wavelength for the laser. Significant supercontinuum occurred and this is most noticeable in the plateau just to the right of the pump wavelength. The power to the supercontinuum fiber was adjusted so that this plateau occurred in the heart of the CO absorption band which goes from approximately 1560 nm to 1600 nm.

Figure 6.5 is a trace of data that was collected by shooting low quality light through the CO-filled cell into singlemode fiber and analyzed using the split pulse approach with no digital averaging.

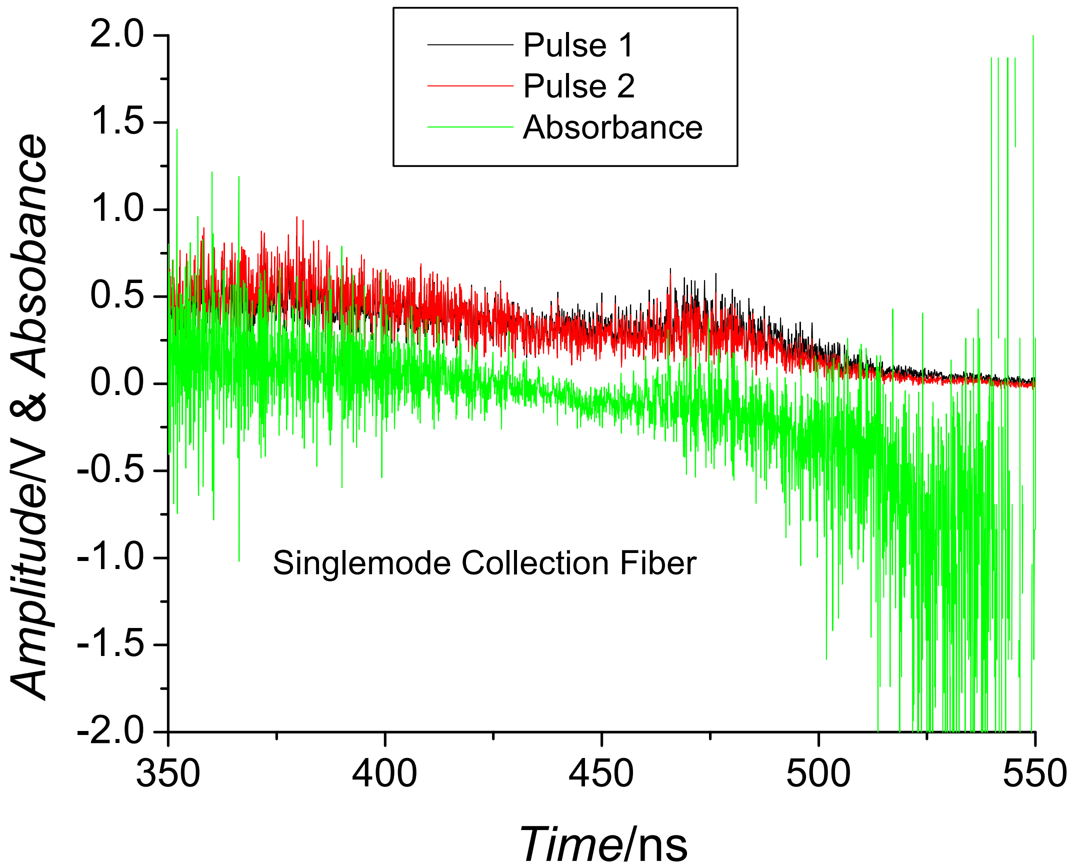

Figure 6.5. CO absorbance – split pulse 0 averages collected in singlemode fiber

The two pulses are seen as black and red and match up reasonably well with each other for this singleshot case. The green trace is the CO absorption that was measured and it is seen that the signal noise case essentially covers up all of the CO absorption lines.

To improve the signal-to-noise ratio, the same signal was averaged 100 times and the results are shown in Figure 6.6.

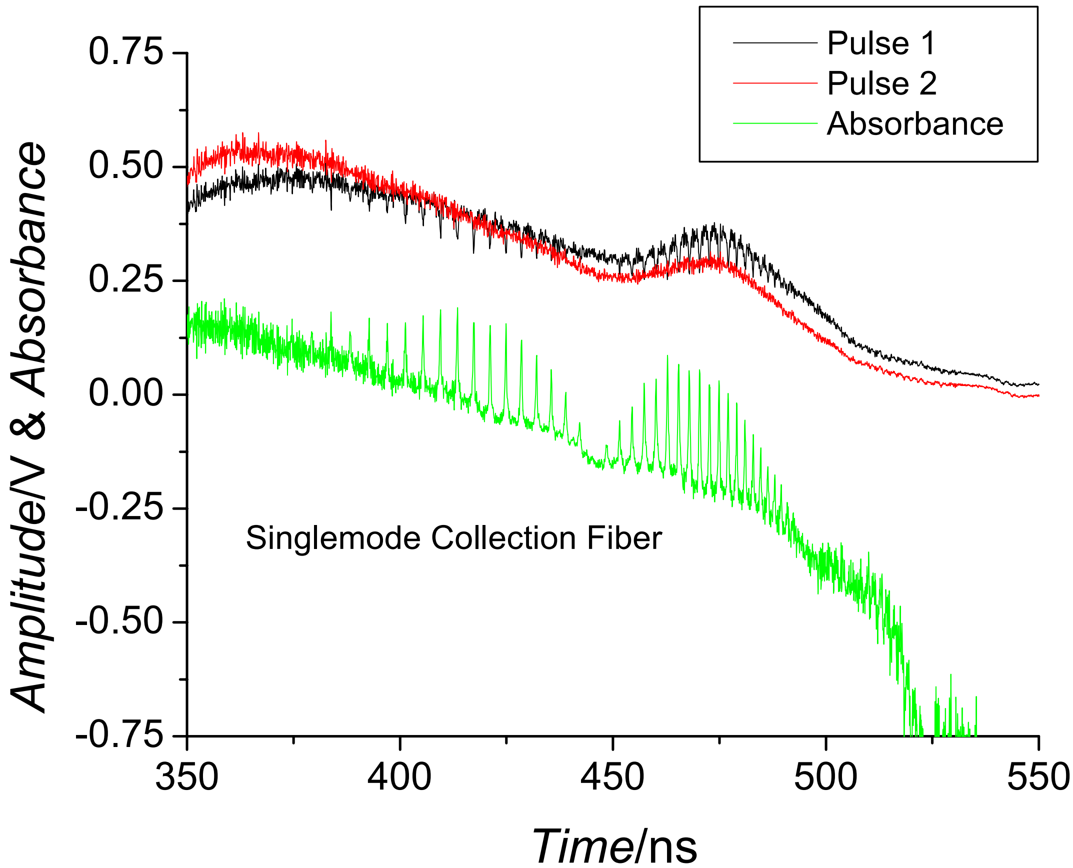

Figure 6.6. CO absorbance – split pulse 100 averages collected in singlemode fiber

From this figure it is easy to identify the black trace as the one that was sent through the CO cell due to the presence of multiple absorption lines. The green trace is again the absorption that was calculated from Beer's Law. For this averaged case, the calculated absorption lines are clearly visible and the absorbance noise between the absorption peaks is around 3%.

Data was also collected using the same split pulse approach with multimode collection fiber. The one advantage that multimode fiber has over singlemode fiber is that it is much larger and allows for much more light to be collected. The singlemode collection fiber was 9 μm as this is the largest fiber can be and still exhibit singlemode behavior in the near to low IR range. The multimode fiber that was used was 62.5 μm as this is the largest fiber that the photoreceiver could resolve. Figure 6.7 shows singleshot CO absorption data that was taken using multimode collection fiber and the split pulse approach.

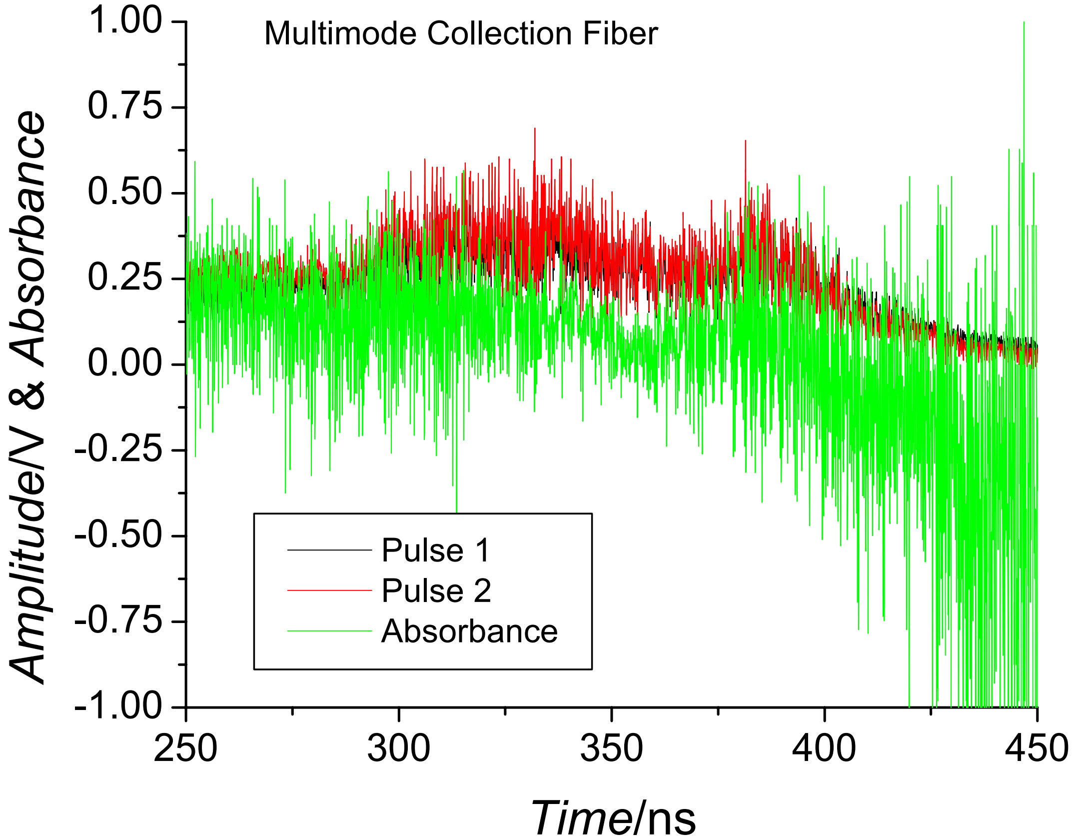

Figure 6.7. CO absorbance – split pulse 0 averages collected in multimode fiber

As before, the red and black traces make up both parts of the split pulse and the green trace is the calculated absorbance. Once again, the noise obscures any absorption lines. Figure 6.8 is a plot of the same thing only averaged 100 times.

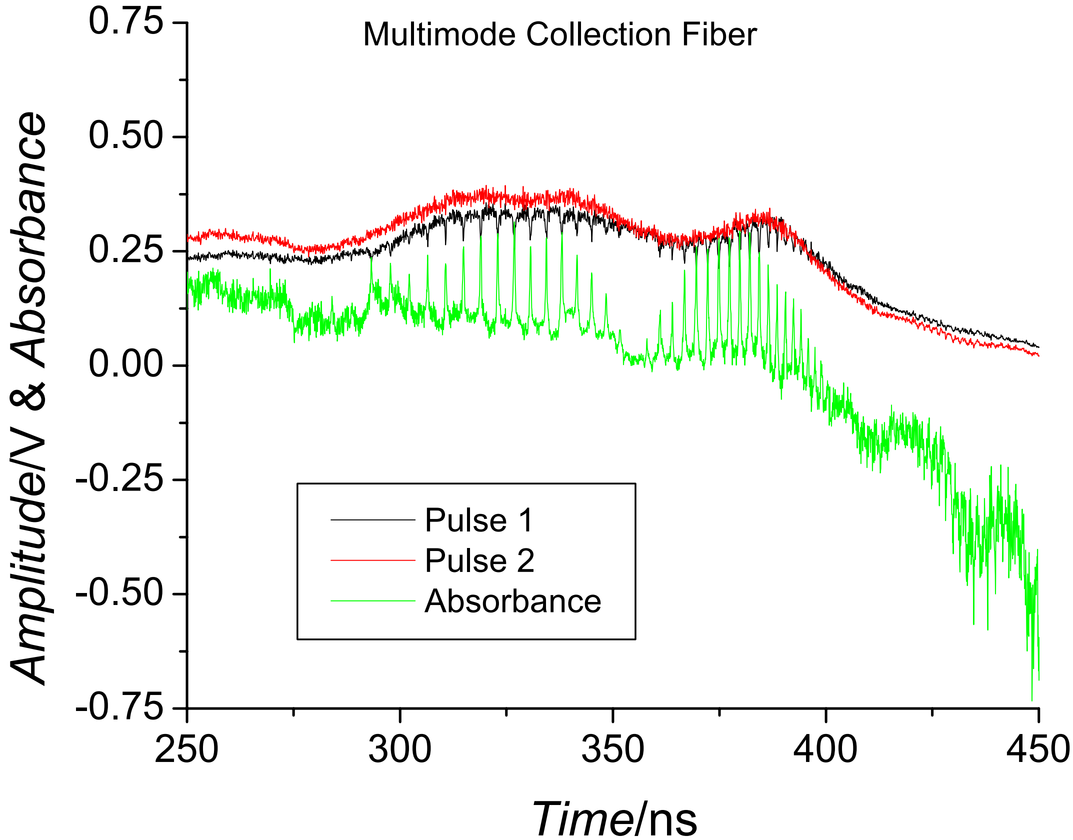

Figure 6.8. CO absorbance – split pulse 100 averages collected in multimode fiber

With averaging the noise pretty much disappears and the CO absorption lines are readily apparent. The absorption noise for this case again is about 3% which is essentially the same as was found when using singlemode collection fiber. This result was somewhat unexpected but nevertheless is very convenient as it is much easier to collect light in multimode fiber as compared to singlemode fiber due to the large difference in area. For this test the multimode fiber had 48 times the area of the singlemode fiber and proved to be much easier to couple light into in the laboratory.

CHAPTER 7 – CONCLUSIONS AND SUMMARY

7.1 Comparison of High Quality Light and Low Quality Light Measurements

From Chapters 5 and 6, it was seen that there is a definite difference between high and low quality light and the setups and techniques that are required to deal with each in a laboratory setting. High quality light requires less equipment and less data processing but is limited by the bandwidth of light that can be classified as high quality. Low quality light typically has a larger bandwidth as it makes up the majority of a spectrum for an optical system but requires more equipment and more work as far as post processing.

For the experiments conducted for this paper both high quality and low quality light trials were able to reach an absorbance error of approximately 3%. The major difference is that no averaging was required for high quality light to reach this accuracy level while the low quality light had to be averaged 100 times to get to 3% error. This result alone is enough to say that employing high quality light is very much preferred to using low quality light for a measurement. It is important to know that even though both the high quality singleshot measurement and low quality measurement averaged 100 times both show CO absorption over approximately 100 ns, the low quality light actually took 500 μs (laser period multiplied by 100) to collect data. So, the singleshot high quality data could be collected in 100 ns every 5 μs while the averaged low quality light required 500 μs to output one trace. For future experiments, if time response is important at all every effort should be make to use high quality light instead of low quality light.

7.2 Comparison of Supercontinuum-based Optical Measurement Techniques to Traditional Measurements Techniques

From the findings presented in this paper, it is seen that the optical techniques for making engine measurements (most notably temperature and pressure) are superior in some important ways as compared to traditional mechanical means. The high quality light data that was presented in Chapter 5 had an error of 3%, was recorded in 100 ns, had a response time of 167 ps, and could be repeated every 5 μs. Even though temperature and pressure was not inferred from the absorption data taken for this paper, spectral information is becoming well-known and any error associated with converting absorption data to temperature and pressure would be much smaller than the error in the absorption data itself. Although the accuracy of the optical data is not as good as that of thermocouples (0.75%) or pressure transducers (0.5%), it would most likely still be acceptable for most applications. With the repetition frequency of this optical system, the crank angle resolution for an engine spinning at 1000 RPM would be 0.03 degrees. For other speeds the resolution would be inversely proportional to engine RPM. The response time and measurement duration for this optical system both are far superior to that of thermocouples and pressure transducers and are the driving reason for continuing work in optical diagnostics.

7.3 Recommendations for Combustion Measurements

Even though the measurements described in this paper were done using a static cell on a laboratory bench, the ultimate goal is to use what was learned in this research for experimental measurements in gas turbines, piston engines, and rocket engines. As explained in Section 7.1 high quality light is preferable to low quality light for making measurements because it has a much faster time response and requires less equipment and post processing. The quicker time response is always desirable and for combustion measurements the fact that high quality light requires less equipment is definitely a good thing as well. The key difference as far as equipment setup is the beamsplitter cube and associated mount for the cube. As any engine will vibrate and move while running it is necessary for alignment purposes to have the cube attached to the engine so it will vibrate as the engine vibrates. If using the split pulse approach with low quality light it is also necessary to try and somehow mount the other leg of the split pulse to the engine so that it will also move as the engine moves. This may sound trivial, but when trying to set up an engine measurement it is always desirable to have the least amount of equipment as possible hanging off the engine. In comparison, a measurement with high quality light could be done with the ring shown in Figure 1.7 by hooking up only an input fiber and a collection fiber. Low quality light measurements would require more work as far as incorporating more equipment so once again high quality would be preferred.

In conclusion, high quality light is recommended for any kind of spectroscopy measurement and for combustion applications in particular because it has a much faster time response for the same accuracy, requires less equipment, and is easier to incorporate into a laboratory setting.

CHAPTER 8 – FUTURE WORK

8.1 Piston Engine Measurements at University of Wisconsin Engine Research Center (UW ERC)

Continuing research with optical sensors incorporating supercontinuum-generated high quality light based on the work done for this thesis is already in progress. High quality supercontinuum light was recently used to measure water absorption in a single cylinder research engine operating in HCCI (homogeneous charge compression ignition) mode. A representative data trace is shown in Figure 8.1.

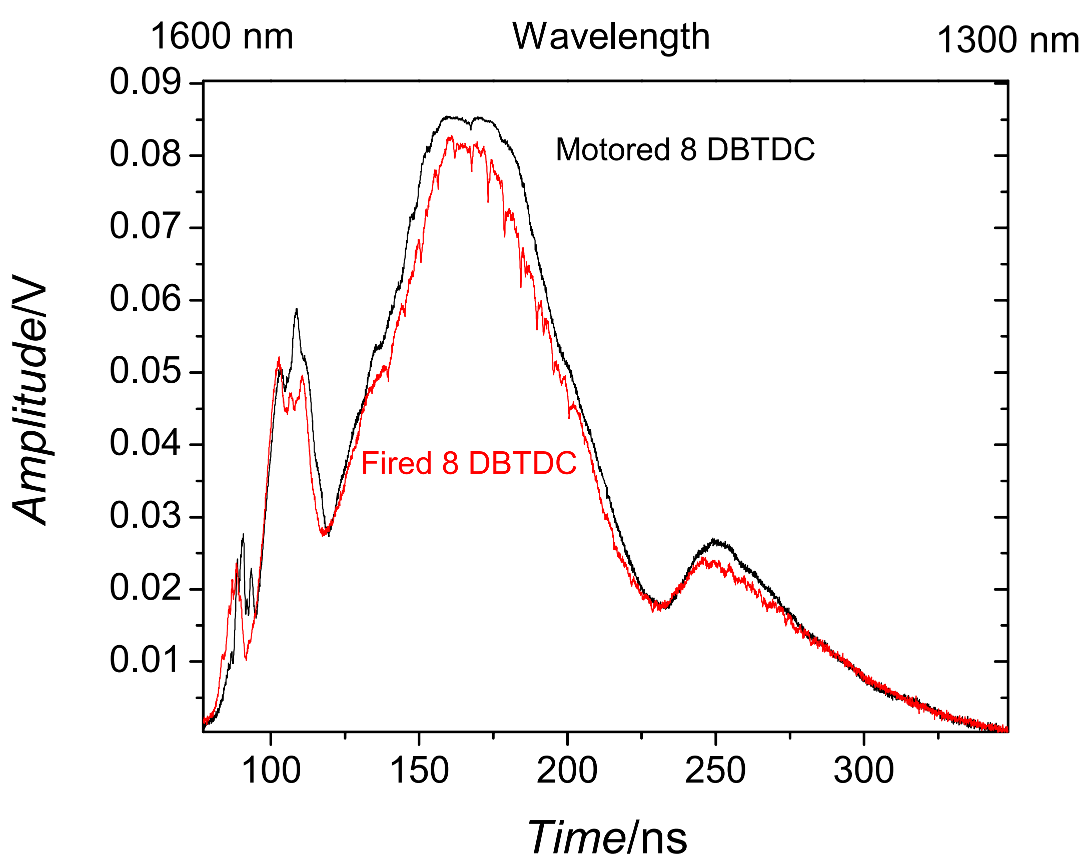

Figure 8.1. Water absorption in an HCCI engine

This is the same figure that was presented in Figure 1.1 illustrating the motivation for this work. In this figure the black trace was recorded while the engine was motored by a dynamometer (not running) and the red trace was recorded while the engine was being fired in HCCI mode. The numerous, narrow decreases in amplitude in the fired trace are water absorption lines and the signal was averaged twenty times to produce the plot above. The wavelength scan for this measurement was from 1300 nm to 1600 nm and without averaging it would have been possible to record this data in approximately 200 ns.

Much work is planned in the future at the UW ERC to build on measurements such as this one and the ideas outlined in this paper. Future goals include limiting interference to increase the bandwidth of high quality light available for a measurement and finding ways to limit signal noise such that singleshot measurements can be taken with a high degree of accuracy.

8.2 Wright-Patterson Air Force Base High Pressure Combustor Research Facility

One major goal for continuing work is to make a measurement at Wright-Patterson Air Force Base's (WPAFB) High Pressure Combustion Research Facility. This facility allows for ground testing of gas turbine combustors at realistic, in-flight conditions. Measurements were attempted at WPAFB but were unsuccessful because there was optical access to only one side of the combustor test section at the time.

A photograph of the WPAFB facility is shown in Figure 8.2.

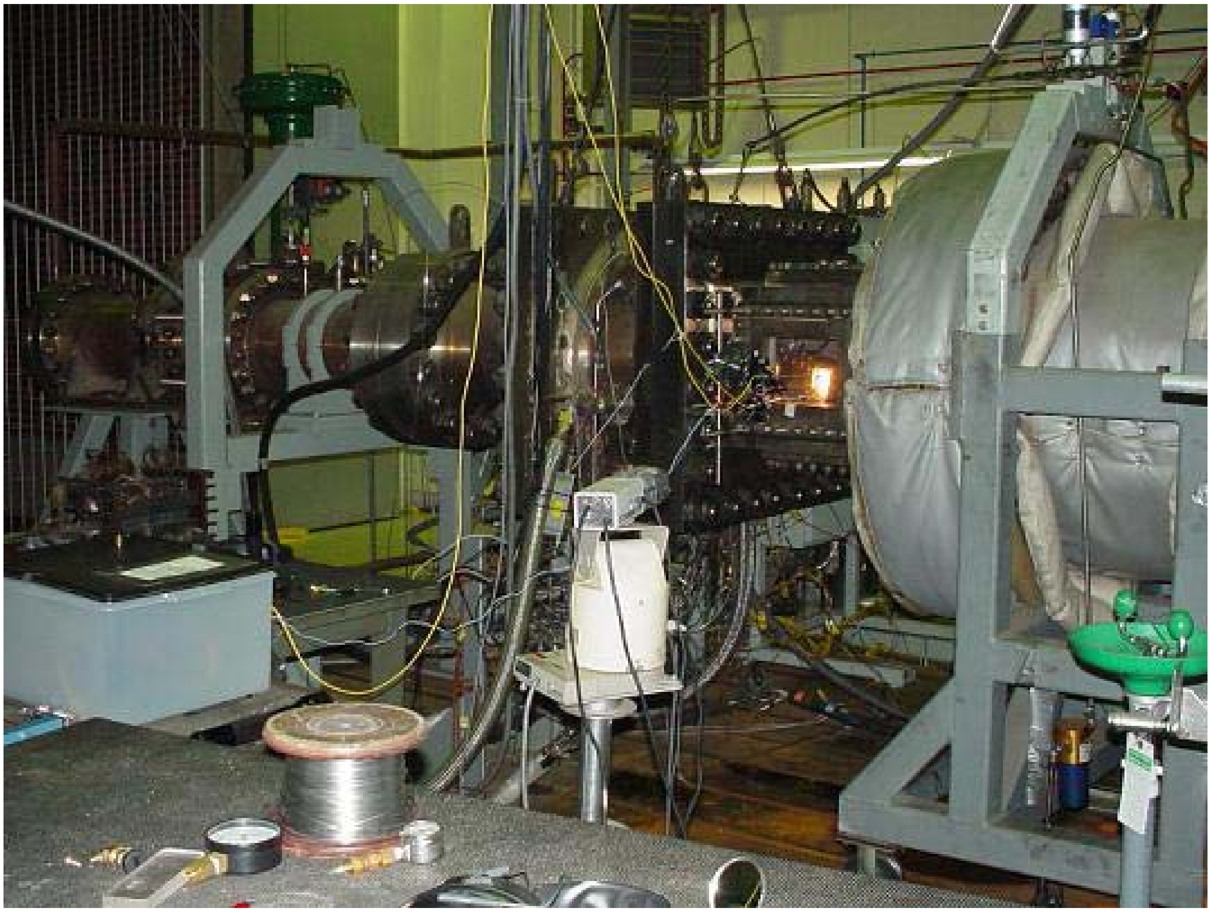

Figure 8.2. High pressure combustion research facility at Wright-Patterson Air Force Base

The combustor is glowing in this picture and the airflow is from right to left as viewed from this angle. When the test rig is up and running the whole building sounds like an airplane taking off from a runway. Figure 8.3 is a close-up of the combustor section.

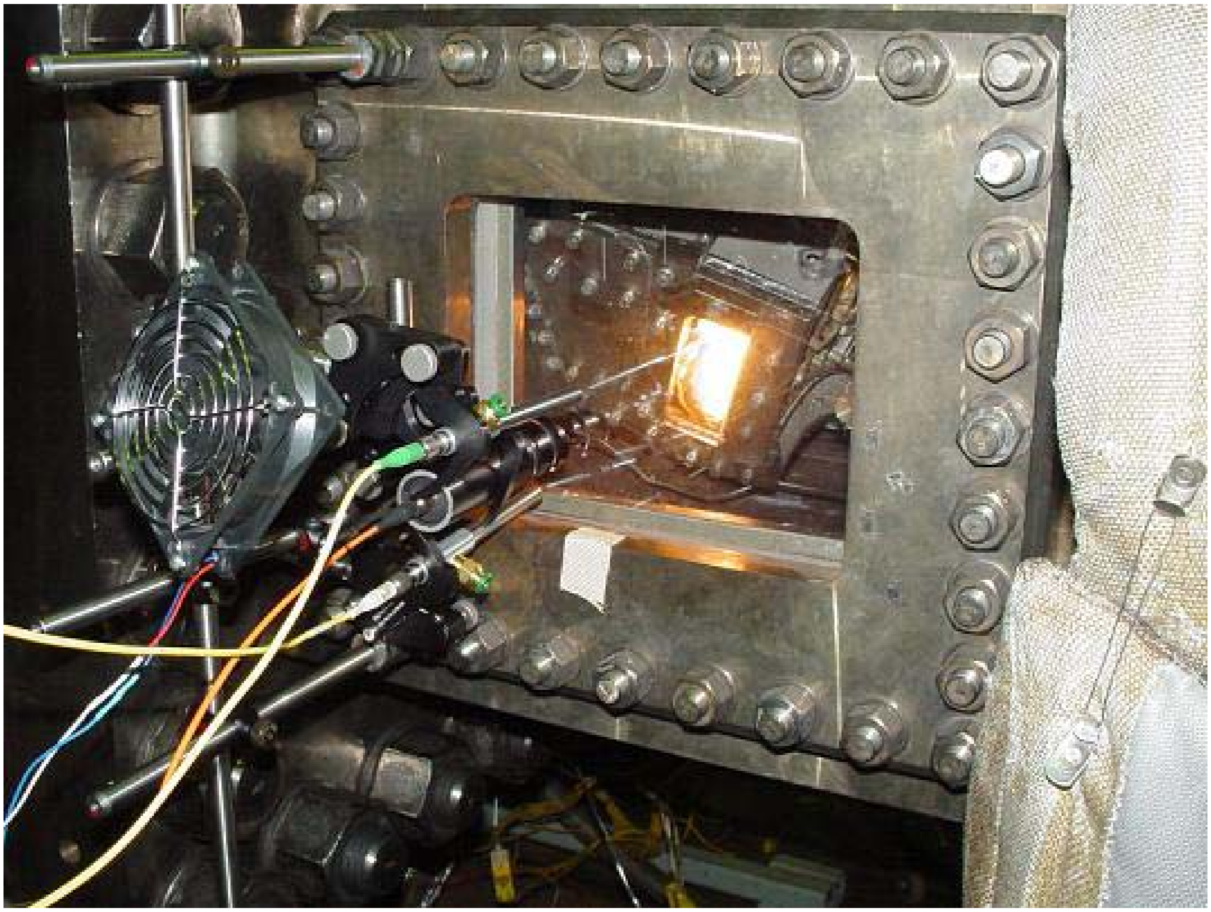

Figure 8.3. Combustor section of WPAFB research facility

As seen in the figure, the test rig utilizes 1/6th of a production combustor from a gas turbine engine. All U.S. turbine manufacturers have tested at WPAFB and these include General Electric, Pratt & Whitney, and Williams International. The research staff at WPAFB has proprietary designs of their own they test as well using this facility.

The optics that were used for the unsuccessful testing are visible in this picture. This test rig allows for easy optical access to the combustion chamber and hopefully testing can be continued when access to both sides of the combustor is available.

8.3 General Purpose Optical Sensor

Although the work outlined in this paper did not produce temperature and pressure data as initially hoped for, much was learned as far as optical sensor development and there is great potential in using what was learned for making engine measurements in the future.

8.3.1 Supercontinuum Light Generation for Use as a Broadband Source

Supercontinuum light generation has been found to be an excellent way to make a broadband light source for taking optical measurements. Wavelength spreads well over 1000 nm have been seen in the laboratory and future work will be centered on filtering techniques to use only the wavelength range(s) of interest and methods to increase the amount of high quality light available from supercontinuum generation. Right now the current thinking is to generate supercontinuum in a short fiber (50 cm or less), disperse the broadband light in a highly dispersive medium such as silicone, filter the light to get only the wavelengths of interest, and couple the light back into SMF-28 singlemode fiber for incorporation into the rest of a measurement system. Future work will be centered on developing a system incorporating these elements.

8.3.2 Combustion Measurement System

There is great potential for making high-speed optical measurements in combustion environments. From the findings in this paper, much was learned about how to build an optical system based on absorption spectroscopy for making engine measurements. As techniques for allowing optical access to piston engines, gas turbines, and rocket engines have already been proven, the main thing holding back the progress of making optical engine measurements is in optical system development. Hopefully with some more work methods can be found to build optical systems that are reliable, high-speed, and accurate so they can be readily applied to achieve a greater understanding of combustion in various applications.

REFERENCES

[1] Sanders,S. T., Kim,T., and Ghandhi,J. B., 2003, "Gas Temperature Measurement during Ignition in an HCCI Engine,"*, Homogeneous Charge Compression Ignition (HCCI), SP-1742*, Anonymous eds.(2003-01-744).

[2] Kranendonk,L. A., Walewski,J. W., Kim,T., and Sanders,S. T., 2005, "Wavelength-Agile Sensor Applied for HCCI Engine Measurements," Proc. Comb. Symp.**, 30**, pp. 1619-1627.

[3] Kong,S. -C, Marriot,C. D., Reitz,R. D., and Christensen,M., 2001, "Modeling and Experiments of HCCI Engine Combustion using Detailed Chemical Kinetics with Multidimensional CFD,"*, Homogeneous Charge Compression Ignition (HCCI), SP-1742*, Anonymous eds., pp.2001-01-1026.

[4] Hanson,R. K., Webber,M. E., and Seitzmann,J. M., 1999-2000, "ME 264: Introduction to Spectroscopic Diagnostics for Gases," .

[5] Iverson,Robert J., 2003"Investigations into the Effects of Intake Charge Preheating and Intake Charge Unmixedness on Gasoline Fueled Homogeneous Charge Compression Ignition Combustion,", University of Wisconsin-Madison, MS Mechanical Engineering.

[6] Hanson,R. K., 1980, "Absorption-Spectroscopy in Sooting Flames using a Tunable Diode-Laser," Appl.Opt.**, 19**(#4Stanford Univ,Dept Mech

Engn/Stanford//Ca/94305 English Article Bibliography Items: 14 Number of times cited: 12 (c) 1999 Inst. For Sci. Info), pp. 482-484.

[7] Wang,J., Sanders,S. T., Jeffries,J. B., and Hanson,R. K., 2001, "Oxygen Measurements at High Pressures with Vertical Cavity Surface-Emitting Lasers," Applied Physics B**, 72**, pp. 865-872.

[8] Kranendonk,L. A., Caswell,A. W., Myers,A. N., and Sanders,S. T., 2002, "Wavelength-Agile Laser Sensors for Measuring Gas Properties in Engines," SAE 2003-01-1116.

[9] Tong,Y. C., Chan,L. Y., and Tsang,H. K., 1997, "Fibre Dispersion Or Pulse Spectrum Measurement using a Sampling Oscilloscope," Electron.Lett.**, 33**(11), pp. 983-985.

[10] Walewski,J. W., and Sanders,S. T., 2004, "High-Resolution Wavelength-Agile Laser Source Based on Pulsed Super-Continua," Appl.Phys.B**, 79**(4), pp. 415-418.

[11] Nishizawa,N., and Goto,T., 2001, "Widely Broadened Super Continuum Generation using Highly Nonlinear Dispersion Shifted Fibers and Femtosecond Fiber Lasers," Jpn.J.Appl.Phys.**, 2**(4B), pp. 365-367.

[12] Walewski,J., Filipa,J., and Sanders,S., 2005, "Super-Continuum Generation in Standard Telecommunication Fibers," Optics Express**, April**.

[13] Sanders,S. T., 2002, "Wavelength-Agile Fiber Laser using Group-Velocity Dispersion of Pulsed Super-Continua and Application to Broadband Absorption Spectroscopy," Applied Physics B**, 75**, pp. 799-802.

[14] Alfano,Robert R., 1989, "The Supercontinuum Laser Source," **, 1**, pp. 458.

[15] Tien,An-Chun, Backus,Sterling, Kapteyn,Henry, Murnane,Margaret, and Mourou,Gerard, 1999, "Short-Pulse Laser Damage in Transparent Materials as a Function of Pulse Duration," Physical Review Letters**, 82**(19), pp. 3883-3884 - 3886.

[16] Wood,Roger M., 2003*, The Power- and Energy-Handling Capability of Optical Materials, Components, and Systems*, The Society of Photo-Optical Instrumentation Engineers, Bellingham, Washington, pp.120.

[17] Walewski,J. W., Filipa,J. A., and Sanders,S. T., 2005, "Optical Interference in Ultra-Fast Spectroscopy. Part I: Fundamental Aspects," J Opt Soc Am B.

[18] Filipa,J. A., Walewski,J. W., and Sanders,S. T., 2004, "Broadband Interference: Part II - Practical Strategies," in preparation.

APPENDIX

A.1 Wright-Patterson Air Force Base High Pressure Combustion Research Facility

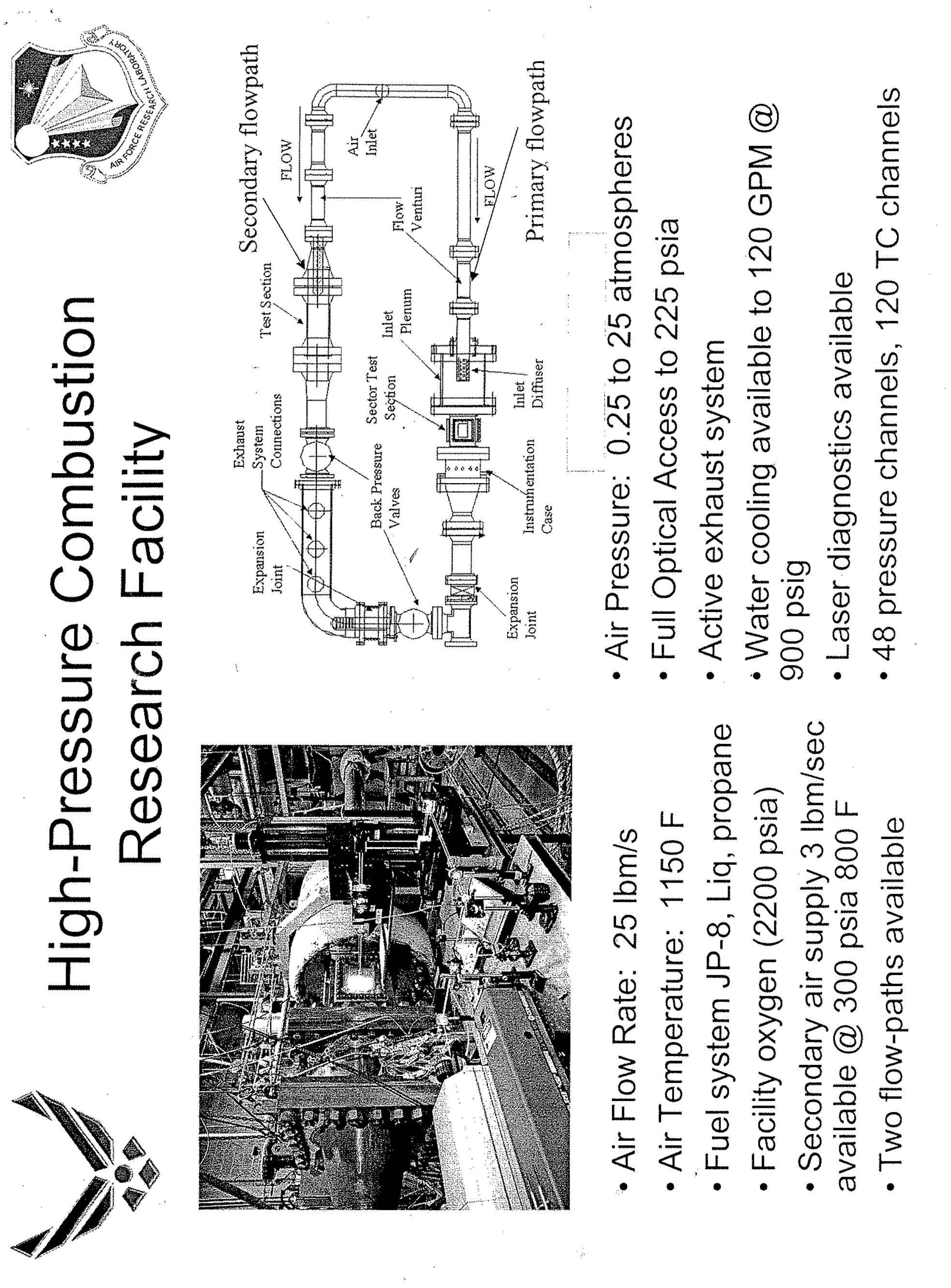

High / Low Pressure Combustion Tunnel Facility

High Pressure Single Cup Rig
- Air Flow Rate: 13 lbs/s; 5.9 kg/s
- Air Temperature: 1100 °F; 593K
- Air Pressure: 45Atms / 0.37 Atms
- No Optical Access 600psi

High / Pressure Sector Rig
- Air Flow Rate: 20 lbs/s; 9 kg/s
- Air Temperature: 1100 °F; 593K
- Air Pressure: 20 / 0.37 Atms
- Optical Access 300psi

Instrumentation
- 96 ~~32~~ Temperatures with TC Rake
- 48 ~~32~~ Pressures
- Emissions gas sampling
- Programmable Logic Controls
- Five Camera Video Documentation

Fuel System Sector & Single Cup
- Two Identical Fuel Systems
- Fuel Type - JP-8, JP - 7, Diesel,
- Flows - 0- 6 GPM Each Leg

8gpm new pumps,

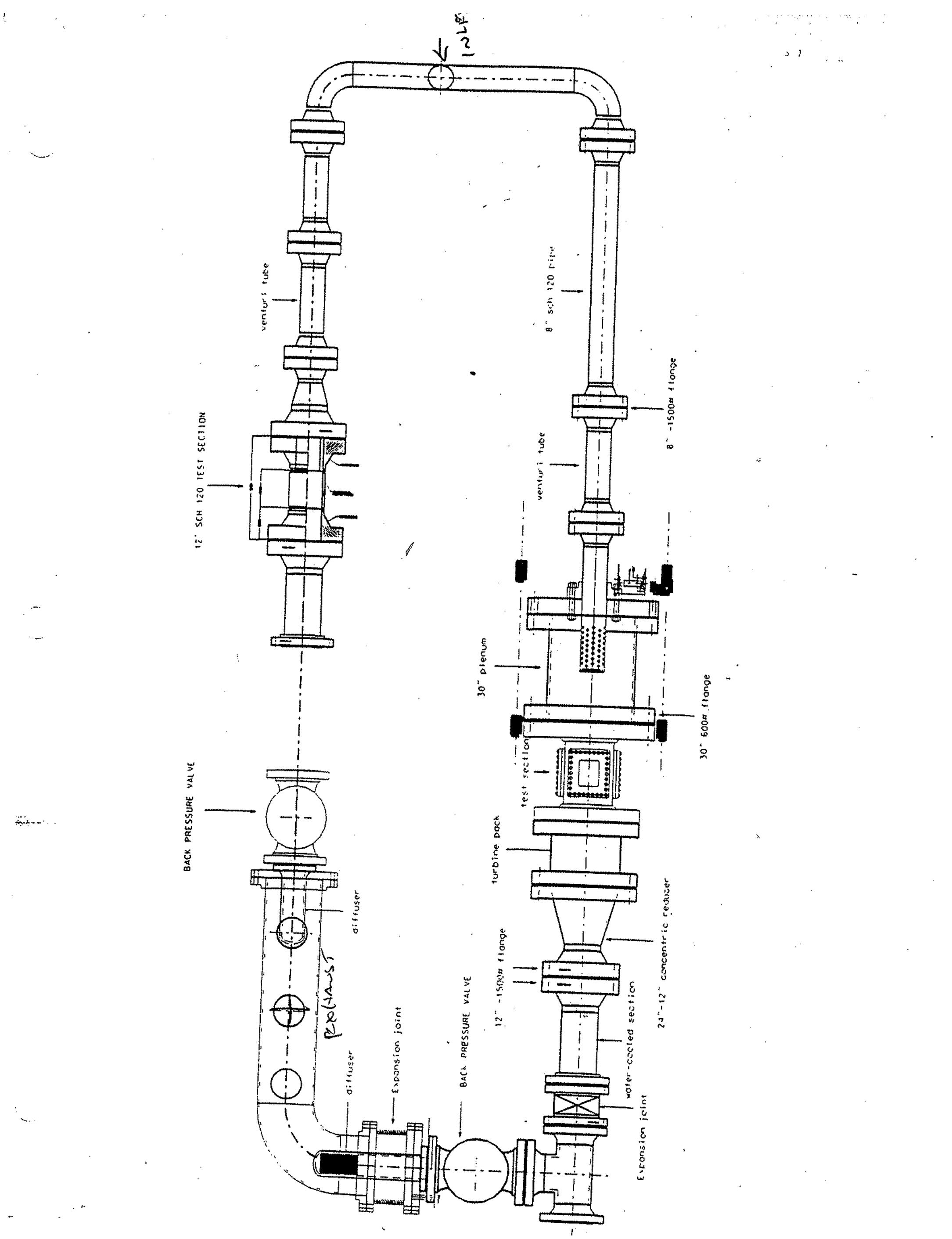
INLET
venturi tube
8" sch 120 pipe
12" SCH 120 TEST SECTION
8" -1500# flange
venturi tube
30" plenum
30" 600# flange
test section
BACK PRESSURE VALVE
turbine pack
diffuser
concentric reducer
12" -1500# flange
24"-12" concentric reducer
EXHAUST
BACK PRESSURE VALVE
water-cooled section
diffuser
Expansion joint
Expansion joint

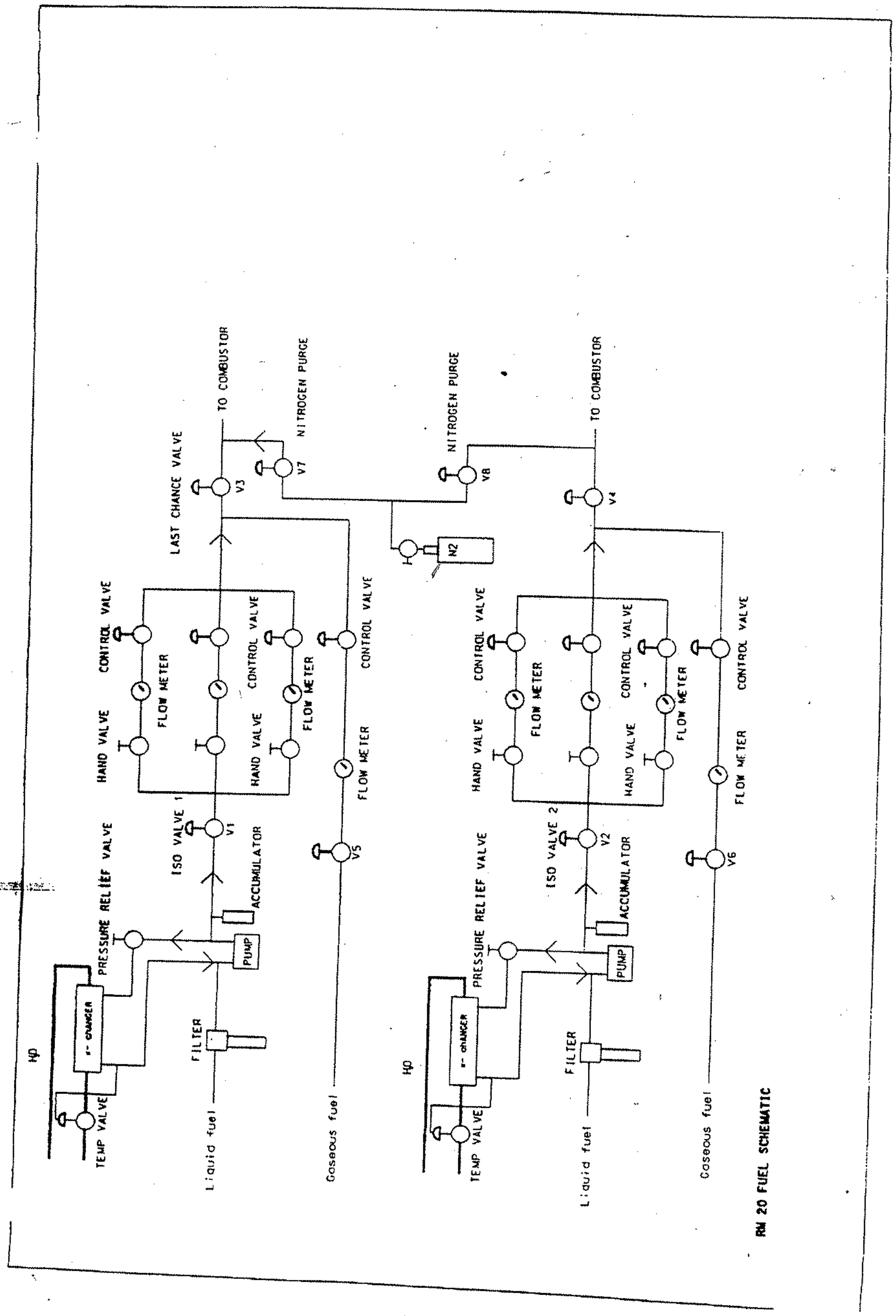

RM 20 FUEL SCHEMATIC

A.2 Sketch of Experimental Setup for CO Absorption Measurements